



TAMPERE UNIVERSITY OF TECHNOLOGY

Simon Ranjith
Quaternions in Joukowski Transformation
Master of Science Thesis

Examiners : Prof.Sirkka-Liisa Eriksson
and Jani Hirvonen (Ph.D)
Examiners and topic approved at the
Faculty of Computing and Electrical
Engineering Council meeting
9th March 2011

Preface

In the Summer of 2010, I started working as a research assistant with the research group ‘Clifford Algebras and Potential Theory’ in the Department of Mathematics, Tampere University of Technology, Finland. My task was to study a conformal map, that is, a Joukowski transformation. This function is unique in the sense that it was seasoned with quaternions. To add to this, the mapping function was subjected to hyperbolic geometry which made the work even more appealing.

Although the implementation was executed during last Summer, most part of the thesis was written in the first four months of the year 2011.

I am grateful to my supervisor Prof. Sirkka-Liisa Eriksson for the opportunity and her guidance during this thesis work. Her kindness is greatly appreciated as well. I also thank Jani Hirvonen, the second examiner, staffs, colleagues in the department for their friendliness, support and assistance.

I am equally thankful to my father Ambrose Jeyabalan and elder brother Emmanuel for their love, support and encouragement. I also express my gratitude to David Holland for proof-reading the text in this report.

As I finish my Masters I should say that this has been a long journey - a span close to nine years since the conception up until now. While I look back at the days that have passed by, the storms I have faced in life, I have no other explanation than to say that He has been on my trail and *is* ever so faithful to keep His Word. I’m indebted to say to Him ‘thank you’.

Life goes on in seasons and rolls on even faster than you can imagine. But I’m excited to know what is in store as I have realized that ‘I’m blessed!’, (Ephesians 1:3).

Simon Ranjith
Tampere, Finland
June 2011

simon.jeyabalan@tut.fi
simonranjith@gmail.com

Contents

Abstract	V
Notations	VI
1 Introduction	1
2 Quaternions	3
2.1 Introduction	3
2.2 Properties of Quaternions	4
2.3 Applications of Quaternions	9
3 Airfoil	10
3.1 Introduction	10
3.2 Nomenclature	10
3.3 Classification	11
3.4 Why use an airfoil?	12
4 Conformal Mapping	13
4.1 Introduction	13
4.2 Joukowski profile in 2-dimension	14
4.3 Joukowski profile in \mathbb{R}^{m+1}	16
4.3.1 Profile in 3-dimension	17
4.3.2 Replacing \mathbb{C} with \mathbb{H}	20
5 Euclidean Geometry	22
5.1 Introduction	22
5.2 Joukowski profile - Euclidean	22
6 Hyperbolic Geometry	27
6.1 Introduction	27
6.2 Hyperbolic models	28

6.2.1	Upper half space model	28
6.2.2	Unit ball model	29
6.2.3	Klein model	29
6.2.4	Hyperboloid model	30
6.3	Joukowski profile - Hyperbolic	31
6.4	Non-Euclidean center in a hyperbolic sphere	34
7	Generalities	37
7.1	Hypermonogenic	37
7.1.1	M.Riesz system in \mathbb{R}^3	37
7.1.2	Modified system in \mathbb{R}^3	38
8	Interactive tools	48
9	Conclusion	51
	Bibliography	53
A	M-files	55
A.1	Joukowski profile in 2-dimension	55
A.2	Joukowski profile in \mathbb{R}^{m+1}	56
A.3	Joukowski profile - Euclidean	58
A.4	Joukowski profile - Hyperbolic	60
A.5	Non-Euclidean center	62
A.6	Test values	63

Abstract

TAMPERE UNIVERSITY OF TECHNOLOGY

Master's Degree Programme in Information Technology

SIMON RANJITH : Quaternions in Joukowski Transformation

Master of Science Thesis, 61 pages, 9 Appendix pages

June 2011

Major: Mathematics

Examiners: Prof.Sirkka-Liisa Eriksson and Jani Hirvonen (Ph.D)

Keywords: Conformal mapping, Quaternions, Joukowski Transformation, Airfoils, Hypermonogenic

Conformal mappings have been exploited for a long time in a number of physical problems arising in aerodynamics, thermal equilibrium, electrostatics, fluid flow and so on. These complex-valued functions are implemented with *just* a single complex variable z . However, in this study, *quaternions* are introduced into a *Joukowski transformation*, a conformal map used in the study of fluid flow around airfoils. Analysis is effected so as to determine the properties of this transformation function and spheres of both Euclidean and hyperbolic geometry are executed in this expedition.

Notations

$ $	<i>Absolute value or modulus</i>
\times	<i>Cross product</i>
\cdot	<i>Dot product</i>
$\ \cdot \ $	<i>Euclidean norm</i>
$\langle \cdot , \cdot \rangle$	<i>Inner product</i>
\int	<i>Integral</i>
\int_{σ}	<i>Integral over the region σ</i>
$\partial/\partial x_i$	<i>Partial derivative with respect to x_i</i>
\sum	<i>Sum</i>
$\alpha, \beta, \gamma, \theta$	<i>Polar or Inclination angles</i>
φ, ψ	<i>Azimuth angles</i>
ζ	<i>Center of an Euclidean sphere</i>
$\hat{\zeta}$	<i>Center of a hyperbolic sphere</i>
λ	<i>Transformation parameter</i>
π	<i>Pi</i>
δ_{kl}	<i>Kronecker symbol</i>
Δ	<i>Laplace operator</i>
Δ_{LB}	<i>Laplace-Beltrami operator</i>
\mathbb{C}	<i>2-dimensional vector space over field of real numbers</i>
$Cl_{0,m}$	<i>2^m-dimensional Clifford algebra over \mathbb{R}</i>
<i>div</i>	<i>Divergence of a vector field</i>
d_h	<i>Hyperbolic distance between any two points</i>
D	<i>Dirac operator</i>
e_i	<i>Orthonormal basis of the Euclidean vector space</i>
<i>grad</i>	<i>Gradient of a scalar field</i>
\mathbb{H}	<i>4-dimensional algebra over field of real numbers</i>
$J(z)$	<i>Joukowski transformation over field of complex numbers</i>
\mathbb{N}	<i>Set of natural numbers</i>
r	<i>Radius of an Euclidean sphere</i>

- r_h *Radius of a hyperbolic sphere*
- \mathbb{R} *Vector space over field of real numbers*
- \mathbb{R}^m *m-dimensional vector space over field of real numbers*
- \mathbb{R}_+^3 *3-dimensional vector space in the Euclidean upper half plane*
- rot* *Curl(cross product) of a vector field*
- $w(q)$ *Joukowski transformation over field of quaternions*

Chapter 1

Introduction

The term “*Conformal mapping*” originated as a consequence of an elementary observation that the composition of two complex functions is also a complex function [17]. This operation is also interpreted as a *complex change of variables* and it is known to preserve angles.

Conformal mappings are widely used in constructing solutions to problems that arise in physical phenomena such as fluid flow, aerodynamics, thermal equilibrium electrostatics and so on.

In our study, we shall examine *Joukowski transformation*, a conformal map used in the study of fluid flow around *airfoils* and in pursuit *quaternions*, a 4-dimensional hypercomplex system are introduced. They replace the complex variable z in the mapping function. Both Euclidean and hyperbolic spheres in 3-dimension are executed and the generated shapes are analyzed. In simple words, we determine the properties of this transformation function.

This report is structured in such a way that the next three chapters are considered as preliminaries followed by results, analysis and then the conclusion. However, a short description of each chapter is given below.

- Chapter 2 briefly describes airfoils. The reader is guided through an outline of the nomenclature and characteristics of airfoils.
- Chapter 3 discusses quaternions and their basic properties. This helps the reader to understand that quaternions form a type of algebra unlike any other. Further, their applications are also pointed out.
- Chapter 4 reflects on conformal mappings. In particular, we shall analyze the Joukowski transformation. A careful study is conducted on the mapping function in 2-dimension and the generalized hypercomplex profile in \mathbb{R}^{m+1} . Further, we

shall also introduce the Joukowski transformation function which depends on quaternions.

- In Chapter 5, the transformations generated as a result of executing an Euclidean sphere in our hypercomplex Joukowski function are exhibited.
- In Chapter 6, the results yielded by implementing a hyperbolic sphere into the mapping function are discussed. Prior to that, a portrait of hyperbolic geometry is given and we shall also elucidate the commonly used mathematical models such as the *Upper half space model*, *Unit ball model*, *Klein* and *the Hyperboloid model*. Finally, an examination is performed to know the whereabouts of the non-Euclidean center in a hyperbolic sphere.
- Chapter 7 presents the Graphical User Interfaces(GUIs) that were designed to visualize the Joukowski transformations. That is to say, their features and instructions on how to handle the tools are explained.
- In chapter 8, we discuss the generalized function theory for *hypermonogenic* functions.
- Chapter 9 summarizes the results of the study and provides suggestions for future work.

Chapter 2

Quaternions

The definitions, propositions and theorems in this chapter are referred from [13], [15], [21] and [22].

2.1 Introduction

Quaternions form a 4-dimensional algebra with the basis elements $1, i, j, k$ and the multiplication defined by

$$i^2 = j^2 = k^2 = -1$$

$$ij = -ji = k$$

$$jk = -kj = i$$

$$ki = -ik = j$$

It was first conceived by the Irish Mathematician *Sir William Rowan Hamilton* in 1843 as extended complex numbers. The novel feature of quaternions is the non-commutative multiplication which is noticed above and this renders quaternions a distinct arithmetic from its real counterpart \mathbb{R}^4 .

The general form of a quaternion is given by

$$q = t + ix + jy + kz$$

where t, x, y, z are real numbers. However, quaternions can be defined in several different, equivalent ways. They can be treated as quadruples of real numbers (t, x, y, z) with suitable arithmetic operations. But these components naturally group themselves into the real part, t , called the *scalar*, and the imaginary part, $ix + jy + kz$, referred to as the *pure quaternion or vector*. Further, a pure quaternion can be identified with a three-dimensional vector v . Thus a quaternion can also be written as (t, v) , with $v = (x, y, z)$.

The algebra of quaternions is denoted by \mathbb{H} (for Hamilton). The vector space \mathbb{C} is a subset of \mathbb{H} . This is achieved by identifying every complex number $t + ix$ with $t + ix + j.0 + k.0$. Therefore the relation $\mathbb{R} \subset \mathbb{C} \subset \mathbb{H}$ is inferred. A quaternion q is called *reduced* if $z = 0$.

2.2 Properties of Quaternions

Addition

The sum of two quaternions is given by

$$\begin{aligned} q_1 + q_2 &= (t_1, v_1) + (t_2, v_2) \\ &= (t_1 + t_2, v_1 + v_2). \end{aligned} \tag{2.1}$$

Multiplication

The quaternion multiplication can be expressed in terms of vector algebra : If $\text{Re } q_1 = t_1$, $\text{Re } q_2 = t_2$, $\text{Im } q_1 = v_1$ and $\text{Im } q_2 = v_2$, then

$$\begin{aligned} q_1 q_2 &= (t_1 + v_1)(t_2 + v_2) \\ &= t_1 t_2 + t_1 v_2 + t_2 v_1 - v_1 \cdot v_2 + v_1 \times v_2. \end{aligned} \tag{2.2}$$

In particular, the product of pure quaternions $q_1 = v_1$, $q_2 = v_2$ is

$$v_1 v_2 = -v_1 \cdot v_2 + v_1 \times v_2. \tag{2.3}$$

where $v_1 \cdot v_2$ is the dot product and $v_1 \times v_2$ is the cross product between the vectors v_1 and v_2 .

Remark

The product of two quaternions

$$q = \begin{pmatrix} t_1 \\ x_1 \\ y_1 \\ z_1 \end{pmatrix} \quad p = \begin{pmatrix} t_2 \\ x_2 \\ y_2 \\ z_2 \end{pmatrix}$$

can also be written as a matrix product:

$$q * p = Q(q) p = \begin{pmatrix} t_1 & -x_1 & -y_1 & -z_1 \\ x_1 & t_1 & -z_1 & y_1 \\ y_1 & z_1 & t_1 & -x_1 \\ z_1 & -y_1 & x_1 & t_1 \end{pmatrix} \begin{pmatrix} t_2 \\ x_2 \\ y_2 \\ z_2 \end{pmatrix} \tag{2.4}$$

or equivalently as

$$q * p = Q(q)p = \begin{pmatrix} t_2 & -x_2 & -y_2 & -z_2 \\ x_2 & t_2 & z_2 & -y_2 \\ y_2 & -z_2 & t_2 & x_2 \\ z_2 & y_2 & -x_2 & t_2 \end{pmatrix} \begin{pmatrix} t_1 \\ x_1 \\ y_1 \\ z_1 \end{pmatrix}. \quad (2.5)$$

Conjugate

The conjugate of the quaternion $q = t + ix + jy + kz$ is defined as

$$\bar{q} = t - ix - jy - kz. \quad (2.6)$$

Thus $\operatorname{Re} q = \frac{1}{2}(q + \bar{q})$ and $\operatorname{Im} q = \frac{1}{2}(q - \bar{q})$.

Modulus

The modulus of q is the real number $|q|$ given by

$$|q|^2 = t^2 + x^2 + y^2 + z^2, \quad |q| = 0. \quad (2.7)$$

Since t, x, y, z are real numbers, $|q|^2 = 0$ if and only if $t = x = y = z = 0$, i.e.

$$|q|^2 = 0 \iff q = 0.$$

The quaternion conjugate and modulus are related to the complex conjugate and modulus in a similar way.

Proposition 2.2.1 *Let q, q_1 , and q_2 be quaternions. Then*

$$(i) \quad q\bar{q} = \bar{q}q = |q|^2. \quad (2.8)$$

$$(ii) \quad \overline{q_1 q_2} = \bar{q}_2 \bar{q}_1. \quad (2.9)$$

$$(iii) \quad |q_1 q_2| = |q_1| |q_2|. \quad (2.10)$$

proof

- (i) If $q = t + v$, then $\bar{q} = t - v$. Therefore by definition, the multiplication of quaternions q and \bar{q} is given by

$$q\bar{q} = (t + v)(t - v) = t^2 + v \cdot v = |q|^2.$$

Similarly, we have

$$\bar{q}q = (t - v)(t + v) = t^2 + v \cdot v = |q|^2.$$

(ii) From (2.2), we get $\overline{q_1 q_2} = t_1 t_2 - t_1 v_2 - t_2 v_1 - v_1 \cdot v_2 - v_1 \times v_2$

$$\begin{aligned}\bar{q}_2 \bar{q}_1 &= (t_2 - v_2)(t_1 - v_1) \\ &= t_2 t_1 - t_2 v_1 - t_1 v_2 - v_2 \cdot v_1 + v_2 \times v_1\end{aligned}$$

Since $v_2 \cdot v_1 = v_1 \cdot v_2$ and $v_2 \times v_1 = -v_1 \times v_2$, it is deduced that $\bar{q}_2 \bar{q}_1 = \overline{q_1 q_2}$.

(iii) Since $|q_2|^2$ is real and commutative with q_1 ,

$$\begin{aligned}|q_1 q_2|^2 &= (q_1 q_2)(\overline{q_1 q_2}) && \text{by (i)} \\ &= q_1 q_2 \bar{q}_2 \bar{q}_1 && \text{by (ii)} \\ &= q_1 |q_2|^2 \bar{q}_1 && \text{by (i)} \\ &= |q_1|^2 |q_2|^2 && \text{by (i)}.\end{aligned}$$

Inverse

The inverse of a non-zero quaternion q is given by

$$q^{-1} = \frac{\bar{q}}{|q|^2}. \quad (2.11)$$

Then from (2.8) we see that

$$qq^{-1} = q^{-1}q = 1. \quad (2.12)$$

Hence the solutions of the systems $ax = b$ and $ya = b$ can be calculated as

$$x = a^{-1}b = \frac{\bar{a}b}{|a|^2}, \quad (2.13)$$

$$y = ba^{-1} = \frac{b\bar{a}}{|a|^2}. \quad (2.14)$$

Unit Quaternion

A unit quaternion is a quaternion which has modulus 1. Any non-zero quaternion q can be written as $q = rs$ where $r = |q|$ is a real number and $s = \frac{q}{|q|}$ is a unit quaternion.

A unit quaternion can also be defined as

$$s = \begin{pmatrix} \cos(\theta/2) \\ u \sin(\theta/2) \end{pmatrix}, \quad (2.15)$$

where θ is a rotation angle and u is a 3-dimensional unit vector.

Proposition 2.2.2 $q^2 = -1$ if and only if q is a pure unit quaternion.

Exponential

The exponential of a quaternion $q = t + ix + jy + kz$ is

$$e^q = e^t(\cos v + I(q) \sin v), \quad (2.16)$$

with $v = \sqrt{x^2 + y^2 + z^2}$ and

$$I(q) = \frac{ix + jy + kz}{\sqrt{x^2 + y^2 + z^2}}. \quad (2.17)$$

In particular $|e^q| = e^{\operatorname{Re} q}$.

Logarithm

The logarithm of a quaternion $q = t + ix + jy + kz$ is

$$\log(q) = \log(|q|) + I \arg q, \quad (2.18)$$

where $I = I(q)$ and

$$\varphi = \arg q = \arccos \frac{t}{\sqrt{x^2 + y^2 + z^2}}. \quad (2.19)$$

Power

The power of a quaternion is defined as

$$q^k = |q|^k(\cos k\varphi + I(q) \sin k\varphi), \quad k \in \mathbb{N}. \quad (2.20)$$

Theorem 2.2.3 (Polar decomposition) *Any quaternion can be written as*

$$q = re^{hv}, \quad (2.21)$$

where r and v are real with $r \geq 0$, and h is a pure unit quaternion.

Matrix description of \mathbb{H}

Any quaternion $q \in \mathbb{H}$ can be written of the form

$$q = \underbrace{(t + ix)}_u + \underbrace{(y + iz)}_w j = u + wj, \quad u = t + ix, \quad w = y + iz. \quad (2.22)$$

We observe that for a complex number $u = t + ix$

$$uj = j\bar{u}. \quad (2.23)$$

Now the product of two quaternions q_1 and q_2 may be computed as

$$\begin{aligned}
 q_1 q_2 &= (u_1 + w_1 j)(u_2 + w_2 j) \\
 &= u_1 u_2 + u_1 w_2 j + w_1 j u_2 + w_1 j w_2 j \\
 &= u_1 u_2 + u_1 w_2 j + w_1 \bar{u}_2 j + w_1 \bar{w}_2 j^2 \\
 &= u_1 u_2 - w_1 \bar{w}_2 + (u_1 w_2 + w_1 \bar{u}_2) j.
 \end{aligned} \tag{2.24}$$

Thus by considering

$$\mathcal{H} = \left\{ \begin{pmatrix} u & w \\ -\bar{w} & \bar{u} \end{pmatrix} : u, w \in \mathbb{C} \right\} \tag{2.25}$$

there exists an algebra isomorphism

$$F : \mathbb{H} \rightarrow \mathcal{H} : q = u + w j \rightarrow \begin{pmatrix} u & w \\ -\bar{w} & \bar{u} \end{pmatrix}$$

and the product yields

$$\begin{aligned}
 \begin{pmatrix} u_1 & w_1 \\ -\bar{w}_1 & \bar{u}_1 \end{pmatrix} \begin{pmatrix} u_2 & w_2 \\ -\bar{w}_2 & \bar{u}_2 \end{pmatrix} &= \begin{pmatrix} u_1 u_2 - w_1 \bar{w}_2 & u_1 w_2 + w_1 \bar{u}_2 \\ -\bar{w}_1 u_2 - \bar{u}_1 \bar{w}_2 & -\bar{w}_1 w_2 + \bar{u}_1 \bar{u}_2 \end{pmatrix} \\
 &= \begin{pmatrix} u_1 u_2 - w_1 \bar{w}_2 & u_1 w_2 + w_1 \bar{u}_2 \\ -\frac{u_1 w_2 + w_1 \bar{u}_2}{(u_1 u_2 - w_1 \bar{w}_2)} & \frac{u_1 u_2 - w_1 \bar{w}_2}{(u_1 u_2 - w_1 \bar{w}_2)} \end{pmatrix}.
 \end{aligned} \tag{2.26}$$

It is concluded that \mathbb{H} is associative, since the multiplication of matrices is associative. Further the following properties are derived:

$$(i) \quad \det \begin{pmatrix} u & w \\ -\bar{w} & \bar{u} \end{pmatrix} = u \bar{u} + w \bar{w} = |u|^2 + |w|^2 = t^2 + x^2 + y^2 + z^2 = |q|^2. \tag{2.27}$$

$$(ii) \quad \text{trace} \begin{pmatrix} u & w \\ -\bar{w} & \bar{u} \end{pmatrix} = u + \bar{u} = t + ix + t - ix = 2t. \tag{2.28}$$

$$(iii) \quad t = \frac{1}{2} \text{trace} \begin{pmatrix} u & w \\ -\bar{w} & \bar{u} \end{pmatrix} = \text{Re } q. \tag{2.29}$$

Theorem 2.2.4 (Rotation) *The rotation of a vector $r \in \mathbb{R}^3$ through an angle θ , around a unit vector $u \in \mathbb{R}^3$ can be computed as*

$$\mathring{r}' = s \mathring{r} \bar{s}, \tag{2.30}$$

where \mathring{r} is the augmented original vector which is of the form $\begin{pmatrix} 0 \\ r \end{pmatrix}$, \mathring{r}' is the augmented rotated vector and s is a unit quaternion as defined in (2.15).

Inverse Rotation

The inverse operation is obtained by taking the conjugate of (2.30)

$$\overset{\circ}{r} = \bar{s}\overset{\circ}{r}'s. \quad (2.31)$$

Theorem 2.2.5 (Conversion to direction cosine matrix) *Rotations can be equivalently represented in terms of direction cosine matrix C as follows:*

$$r' = Cr. \quad (2.32)$$

A unit quaternion is transformed into an equivalent direction cosine matrix using the following expression:

$$C = \begin{pmatrix} t^2 + x^2 - y^2 - z^2 & 2(xy - tz) & 2(xz + ty) \\ 2(xy + tz) & t^2 - x^2 + y^2 - z^2 & 2(yz - tx) \\ 2(xz - ty) & 2(yz + tx) & t^2 - x^2 - y^2 + z^2 \end{pmatrix}. \quad (2.33)$$

2.3 Applications of Quaternions

Quaternions have been a revolution since their introduction to computer graphics at SIGGRAPH (Special Interest Group on GRAPHics and Interactive Techniques) in 1985 and are used in several applications lately. The list includes computer graphics, physically based modeling, constraint systems, user interfaces and so on. For the most part, they are used as coordinates for rotations and orientations.

Quaternions are distinctive as compared to any of its competitors. That is to say, they are known to compete very well both with general co-ordinates such as matrices and with other special co-ordinates such as Euler angles. This is because quaternion implementation is found to be simpler, cheaper and better behaved [20].

Chapter 3

Airfoil

3.1 Introduction

The cross sectional shape of an airplane wing or blade (of a propeller, rotor or turbine) or sail is called an *Airfoil*. Obviously airfoils are used in a wide range of physical applications. Airfoil shapes were first developed by *Horatio F. Phillips* in 1884. He carried out the first serious wind-tunnel experiments on airfoils. In 1902, the *Wright brothers* unfolded relatively efficient airfoil shapes after conducting their own wind-tunnel tests and this contributed to their first successful flight in 1903. However, these airfoil designs were based on their particular requirements. In the early 1930s, the National Advisory Committee for Aeronautics (NACA) - the forerunner of National Aeronautics and Space Administration (NASA) - constructed several airfoil shapes that are in use even today.

In order to know why these complicated (often) non-symmetric geometries are implemented in real-life machines requires a proper understanding of their geometric definitions and it is briefly described in the next section.

3.2 Nomenclature

Consider the diagram in fig.3.1 that represents the shape of an airfoil geometrically. The few common parameters used in the nomenclature of an airfoil are:

- (i) *Chord line* - The straight line drawn from the leading edge to the trailing edge is the chord line. The chord line cuts the airfoil into upper and lower surfaces and is typically used to measure airfoil length.
- (ii) *Mean Camber line* - A curve halfway between the upper and lower surfaces.

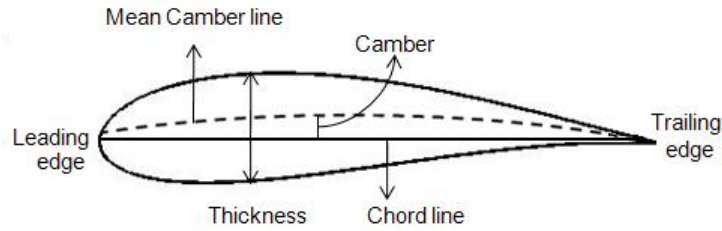


Figure 3.1: Diagram of an airfoil

- (iii) *Camber* - The maximum distance between the Mean Camber line and the chord line is called the camber, which is the measurement of the curvature of an airfoil. High camber means high curvature of the airfoil.
- (iv) *Thickness* - The maximum distance between the upper and lower surface is the thickness of an airfoil.

The above parameters play a key role in an aerodynamic performance and by varying them a family of airfoil sections can be generated. Thus, airfoils can be of varying combinations of thickness and camber depending on their use.

3.3 Classification

In general, the geometry of an airfoil can be classified into two types:

- (i) Symmetric airfoil
- (ii) Non-symmetric airfoil

If the camber line falls on top of the chord line, then the airfoil is symmetrical. As a consequence, the upper surface is the mirror image of the lower surface about the chord line. If the camber line lies either above (*positive camber*) or below (*negative camber*) the chord line, then the airfoil is asymmetric and the upper surface is not a mirror image of the lower surface.

However, the different airfoil shapes developed by NACA in the 1930s were identified with a logical numbering system. As an example, the first family of airfoils was the *four digit* series such as NACA 2412 airfoil [2]. The first digit refers to the maximum camber that is 2% of the chord length in our example. The second digit is the location of the maximum camber along the chord line from the leading edge. This denotes that the maximum camber is located at 4/10 of the chord length from the leading edge.

Finally, the last two digits describe the maximum thickness. In our case, it is 12% of the chord length.

3.4 Why use an airfoil?

The objective of an airfoil is to obtain the necessary lift to sustain an airplane in the air. Of course, a flat plate can perform a similar task. But the outcome is lift but with excessive drag. In the 1800s, *Sir George Cayley* and *Otto Lilienthal* demonstrated that curved surfaces generate more lift and less drag than flat surfaces [8]. Since then more changes and improvements were made to a curved surface through experimentation and this included the desirability of a rounded leading edge and a sharp trailing edge.

Chapter 4

Conformal Mapping

4.1 Introduction

Conformal mapping is a mathematical technique in which complicated geometries are transformed into simpler geometries by a mapping function. It preserves the angles and orientation of the original geometry [10]. In the field of fluid dynamics, conformal mapping plays a significant role in modeling and analyzing the flow of fluid around aircraft wings.

Let us start with an example to get an impression of how this technique works. Consider a complex plane z as in Figure 4.1a. The co-ordinates in this plane are of the form $z = x + iy$. The vertical lines represent equipotential curves given by $\phi = x$ and the horizontal lines represent the stream lines given by the function $\psi = iy$.

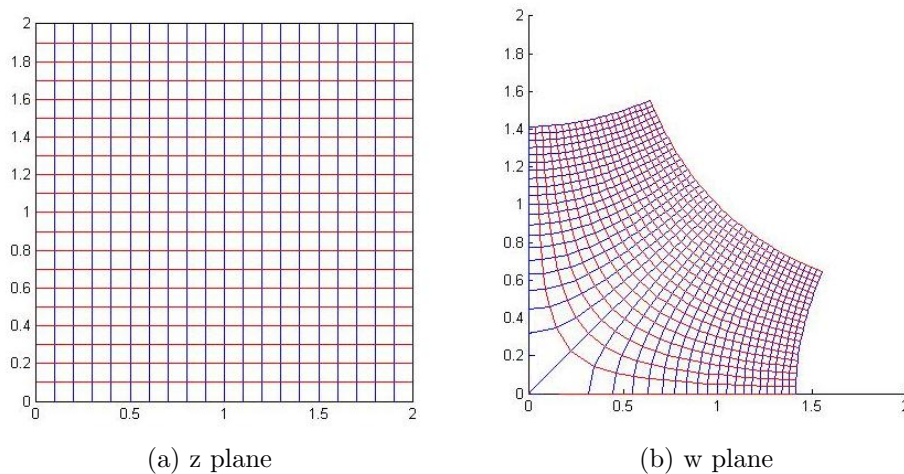


Figure 4.1: An example of conformal mapping

It is seen that a simple uniform fluid flow is transformed from a complex plane z

into a complex plane w through the function $w = \sqrt{z}$. The variables x and y in the z plane are transformed to new variables u and v in the w plane. Though the shape of the streamlines are changed, the angles between the set of curves remain perpendicular. This is an essential feature of conformal mapping. In case of a complex function that models a right circular cylinder in plane z , an appropriate transformation function can be used to obtain airfoils in plane w . The most commonly used function in aerodynamics applications is the *Joukowski transformation*. It was proposed by the Russian aero- and hydro-dynamics researcher *Nikolai Zhukovskii* (*Joukowski*).

$$w(z) = z + \frac{\lambda^2}{z}, \quad (4.1)$$

where λ is the transformation parameter that determines the resulting shape of the transformation function.

4.2 Joukowski profile in 2-dimension

Consider a circle in the z plane described by the equation

$$z = re^{i\theta}, \quad (4.2)$$

where r is the radius of the circle and θ ranges from 0 to 2π . Under the Joukowski mapping,

$$w(z) = z + \frac{\lambda^2}{z} = re^{i\theta} + \frac{\lambda^2}{re^{i\theta}}.$$

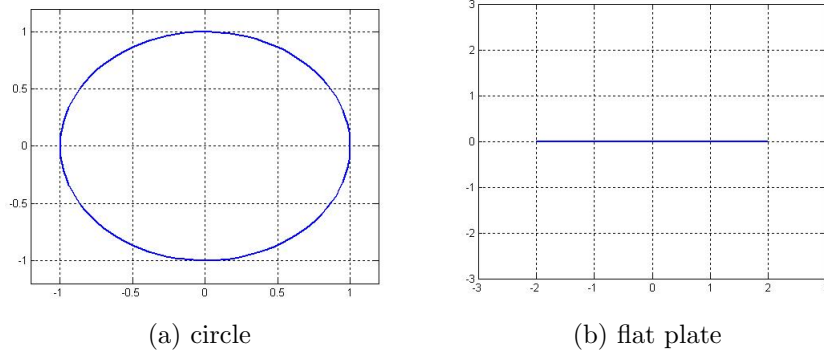


Figure 4.2: A circle of radius $r = 1$ and center at the origin in z plane is transformed to a flat plate in the w plane of length $4r$.

It follows that for $\lambda = r$, the mapping becomes

$$w(z) = r(e^{i\theta} + e^{-i\theta}) = 2r \cos \theta. \quad (4.3)$$

In this case, the Joukowski transformation maps a circle of radius r to a flat plate or a straight line entirely on the real axis in the w plane from $-2r$ to $2r$. This is shown in Figure 4.2b. On the other hand, for values of λ either larger or smaller than r , the circle is mapped to an ellipse as shown in Figure 4.3.

$$w(z) = z + \frac{\lambda^2}{z} = re^{i\theta} + \frac{\lambda^2}{r}e^{-i\theta} = \left(r + \frac{\lambda^2}{r}\right) \cos \theta + i\left(r - \frac{\lambda^2}{r}\right) \sin \theta. \quad (4.4)$$

If $x = \left(r + \frac{\lambda^2}{r}\right) \cos \theta$ and $y = \left(r - \frac{\lambda^2}{r}\right) \sin \theta$, then this can be written as

$$\frac{x^2}{\left(r + \frac{\lambda^2}{r}\right)^2} + \frac{y^2}{\left(r - \frac{\lambda^2}{r}\right)^2} = 1 \quad (4.5)$$

which is an equation of an ellipse.

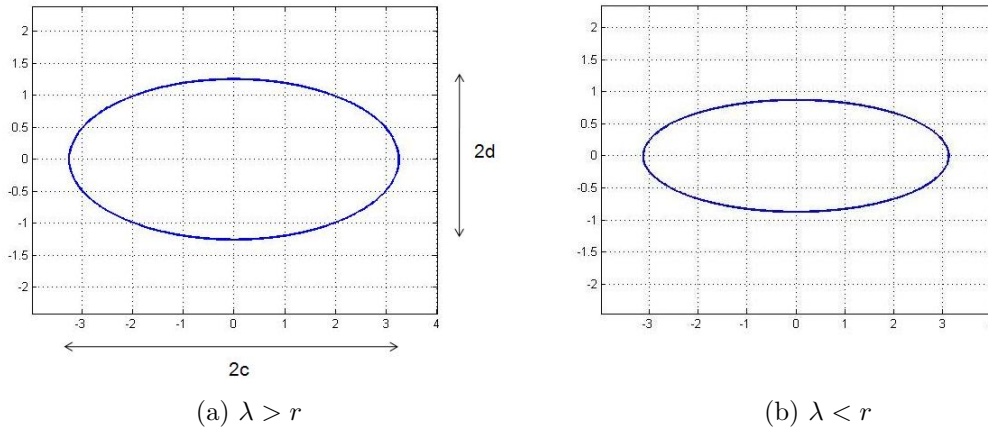


Figure 4.3: Ellipses of axes length $2c$ and $2d$ in the w plane.

The semi-axes of the ellipse are given by

$$c = r + \frac{\lambda^2}{r}, \quad d = r - \frac{\lambda^2}{r}. \quad (4.6)$$

The shape of an airfoil is obtained by considering the circle in z plane with a center that is offset from the origin. In this case the transformation parameter λ is given by

$$\lambda = r - |s|$$

where r is the radius and s is the co-ordinates of the center of the circle. If the center of the circle is offset along the real axis x , a symmetrical airfoil is obtained. If the centre is also offset on the y axis then the transformation results in a cambered airfoil. Thus the x co-ordinate of the center determines the thickness and the y co-ordinate determines the curvature of the transformed airfoil [10].

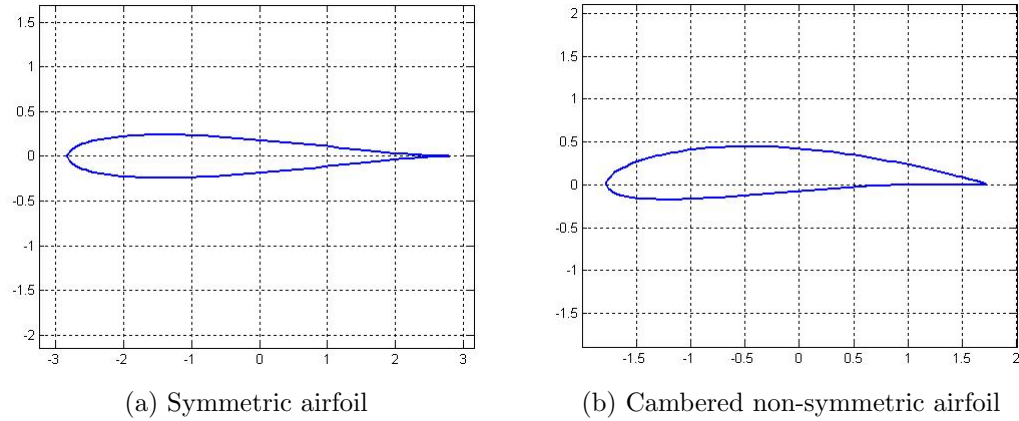


Figure 4.4: Airfoils

4.3 Joukowski profile in \mathbb{R}^{m+1}

Prior to briefing the hypercomplex analogues of the Joukowski transformation let us review some of the elementary concepts of the geometric algebra.

Preliminaries

Let $\{e_1, e_2, \dots, e_m\}$ be an orthonormal basis of the Euclidean vector space \mathbb{R}^m with a non-commutative product according to the multiplication rules

$$e_k e_l + e_l e_k = -2\delta_{kl}, \quad k, l = 1, \dots, m, \quad (4.7)$$

and δ_{kl} is the Kronecker delta. The set of elements $\{e_A : A \subset \{1, \dots, m\}\}$ formed by

$$e_A = e_{h_1} e_{h_2} \dots e_{h_r}, \quad 1 \leq h_1 \leq \dots \leq h_r \leq m, \quad e_\emptyset = e_0 = 1,$$

form a basis of the 2^m -dimensional Clifford algebra $Cl_{0,m}$ over \mathbb{R} .

Let \mathbb{R}^{m+1} be embedded in $Cl_{0,m}$ by identifying an element $(x_0, x_1, \dots, x_m) \in \mathbb{R}^{m+1}$ with

$$x = x_0 + \underline{x}, \quad \text{where } \underline{x} = e_1 x_1 + \dots + e_m x_m.$$

x is called a *para-vector* which implies that it is comprised of an *0-vector* + *1-vector*.

The conjugate of x is $\bar{x} = x_0 - \underline{x}$ and the norm $|x|$ of x is given by

$$|x| := \sqrt{x\bar{x}} = \sqrt{\bar{x}x} = \left(\sum_{k=0}^m x_k^2 \right)^{1/2}.$$

We consider $Cl_{0,m}$ -valued functions of the form

$$f(x) = \sum_A f_A(x) e_A, \quad f_A(x) \in \mathbb{R}$$

as mappings

$$f : \Omega \subset \mathbb{R}^{m+1} \mapsto Cl_{0,m}.$$

If f is a solution of the Cauchy-Riemann system $Df = 0$ ($fD = 0$) where

$$D = \frac{\partial}{\partial x_0} + \partial \underline{x} \quad \text{for } \partial \underline{x} := e_1 \frac{\partial}{\partial x_1} + \cdots + e_m \frac{\partial}{\partial x_m},$$

then f is called a left(right) monogenic function or left(right) holomorphic.

A generalized hypercomplex Joukowski transformation in \mathbb{R}^{m+1} ($m \geq 1$) presented in [14] is given by

$$w(x) = w(x_0 + \underline{x}) = \frac{m}{m+1} (P^m(x) - E^m(x)), \quad (4.8)$$

where

- $P^m(x) = x_0 + \frac{1}{m} \underline{x}$, a left and right monogenic linear function with hypercomplex derivative $(P^m(x))' \equiv 1$, and
- $E^m(x) = \frac{\bar{x}}{|x|^{m+1}}$, a fundamental solution of the corresponding Cauchy-Riemann system.

Remark: The above transformation function is based on the following Joukowski profile:

$$\tilde{w} = \frac{1}{2} \left(z - \frac{1}{z} \right), \quad z = x_0 + ix_1 \in \mathbb{C} \setminus \{0\}.$$

4.3.1 Profile in 3-dimension

Let us study the case where $m = 2$. The corresponding transformation deduced from (4.8) is

$$w(x) = w(x_0 + \underline{x}) = \frac{2}{3} (P^2(x) - E^2(x)). \quad (4.9)$$

Consider the spherical co-ordinates

$$x_0 = r \sin \varphi, \quad x_1 = r \cos \varphi \cos \theta, \quad x_2 = r \cos \varphi \sin \theta, \quad (4.10)$$

with $r = |x| > 0$, the radius of the sphere, $-\pi \leq \theta \leq \pi$, and $-\pi/2 \leq \varphi \leq \pi/2$.

Let $x = x_0 + \underline{x} = x_0 + x_1 e_1 + x_2 e_2$. Now the Joukowski transformation in \mathbb{R}^3 inferred from (4.9) by implementing the above parameters, can be written in terms of spherical co-ordinates

$$w_0 = \frac{2}{3} \left(r - \frac{1}{r^2} \right) \sin \varphi, \quad w_1 = \frac{2}{3} \left(\frac{r}{2} + \frac{1}{r^2} \right) \cos \varphi \cos \theta, \quad w_2 = \frac{2}{3} \left(\frac{r}{2} + \frac{1}{r^2} \right) \cos \varphi \sin \theta. \quad (4.11)$$

Further (4.11) can be formulated as

$$\begin{aligned} \frac{w_0^2}{\left(\frac{2}{3}\left(r - \frac{1}{r^2}\right)\right)^2} + \frac{w_1^2}{\left(\frac{2}{3}\left(\frac{r}{2} + \frac{1}{r^2}\right)\right)^2} + \frac{w_2^2}{\left(\frac{2}{3}\left(\frac{r}{2} + \frac{1}{r^2}\right)\right)^2} &= \sin^2 \varphi + \cos^2 \varphi \cos^2 \theta + \cos^2 \varphi \sin^2 \theta \\ &= \sin^2 \varphi + \cos^2 \varphi (\cos^2 \theta + \sin^2 \theta) \\ &= \sin^2 \varphi + \cos^2 \varphi \\ &= 1. \end{aligned}$$

This is an equation of an ellipsoid in \mathbb{R}^3 with $a = \frac{2}{3}\left(\frac{r}{2} + \frac{1}{r^2}\right)$ as the equatorial radius and $b = \frac{2}{3}\left(r - \frac{1}{r^2}\right)$ as the polar radius. Thus, it can be said that 3-dimensional spheres are transformed into ellipsoids.

The geometrical transformations generated with radius $r = |x| \geq 1$ are listed in the following proposition.

Proposition 4.3.1 *Consider the generalized Joukowski transformation(4.9) in \mathbb{R}^3 . Then,*

- (i) *The unit sphere $r = |x| = 1$ is mapped into $w = \cos \varphi (\cos \theta e_1 + \sin \theta e_2)$, i.e., the 2-folded S^1 , including its interior, in the hyperplane $w_0 = 0$.*
- (ii) *A sphere of radius $r = |x|$ and $1 < r < \sqrt[3]{4}$ is mapped onto an oblate spheroid.*
- (iii) *A sphere of radius $|x| = \sqrt[3]{4}$ is mapped onto a sphere of radius $\frac{1}{\sqrt[3]{2}}$.*
- (iv) *A sphere of radius $|x| = r > \sqrt[3]{4}$ is mapped onto a prolate spheroid with*
 - *equatorial radius $a < 1$ for spheres of radius $\sqrt[3]{4} < r < 1 + \sqrt{3}$;*
 - *equatorial radius $a = 1$ for a sphere of radius $r = 1 + \sqrt{3}$;*
 - *equatorial radius $a > 1$ for spheres of radius $r > 1 + \sqrt{3}$.*

These geometries are observed by direct inspection of (4.11).

Proposition 4.3.2 *Let $r > \sqrt[3]{4}$, then the generalized Joukowski transformation (4.9) in \mathbb{R}^3 is orientation preserving and 4-quasiconformal.*

Proof. Refer [14].

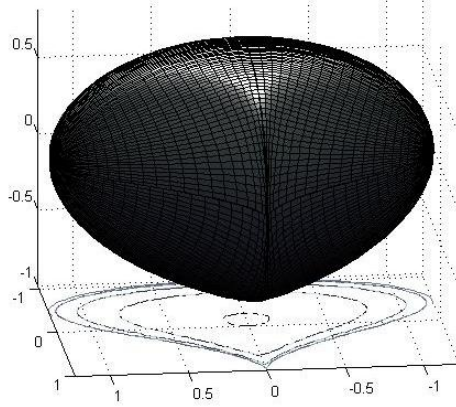


Figure 4.5: 3D Airfoil - rear view

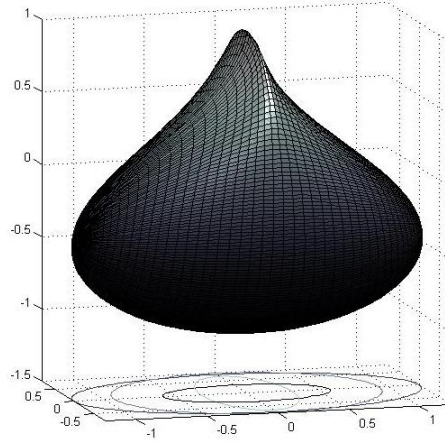


Figure 4.6: 3D Airfoil - side view

Besides, by considering the following co-ordinates

$$x_0 = (1 + r) \sin \varphi, \quad x_1 = -r + (1 + r) \cos \varphi \cos \theta, \quad x_2 = (1 + r) \cos \varphi \sin \theta, \quad (4.12)$$

with $r = |x| > 0$, the radius of the sphere, $-\pi \leq \theta \leq \pi$, and $-\pi/2 \leq \varphi \leq \pi/2$ and substituting in (4.9) yields Joukowski airfoils. These airfoils are shown in Figure 4.5 and 4.6 respectively .

$$\begin{aligned} w = & \frac{2}{3} (1 + r) \sin \varphi \left(1 - (r^2 + (1 + r)^2 - 2r(1 + r) \cos \varphi \cos \theta)^{-3/2} \right) e_0 \\ & + \frac{2}{3} (-r + (1 + r) \cos \varphi \cos \theta) \left(\frac{1}{2} + (r^2 + (1 + r)^2 - 2r(1 + r) \cos \varphi \cos \theta)^{-3/2} \right) e_1 \\ & + \frac{2}{3} (1 + r) \cos \varphi \sin \theta \left(\frac{1}{2} + (r^2 + (1 + r)^2 - 2r(1 + r) \cos \varphi \cos \theta)^{-3/2} \right) e_2. \end{aligned} \quad (4.13)$$

A slight adjustment in view of the above spherical co-ordinates

$$x_0 = (1+r) \sin \varphi, \quad x_1 = (1+r) \cos \varphi \cos \theta, \quad x_2 = -r + ((1+r) \cos \varphi \sin \theta), \quad (4.14)$$

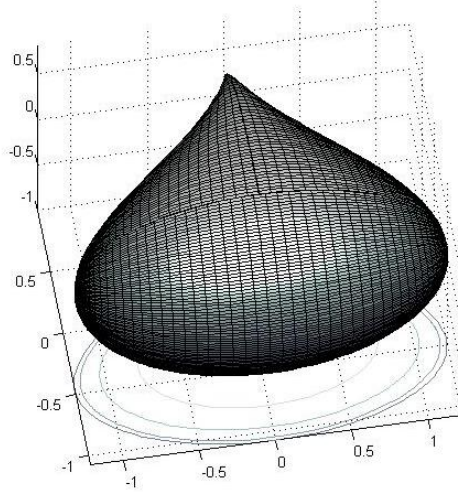


Figure 4.7: 3D Airfoil - top view

results in the following transformation which generates an airfoil as in Figure 4.7

$$\begin{aligned} w = & \frac{2}{3} (1+r) \sin \varphi \left(1 - (r^2 + (1+r)^2 - 2r(1+r) \cos \varphi \sin \theta)^{-3/2} \right) e_0 \\ & + \frac{2}{3} (1+r) \cos \varphi \cos \theta \left(\frac{1}{2} + (r^2 + (1+r)^2 - 2r(1+r) \cos \varphi \sin \theta)^{-3/2} \right) e_1 \\ & + \frac{2}{3} (-r + ((1+r) \cos \varphi \sin \theta)) \left(\frac{1}{2} + (r^2 + (1+r)^2 - 2r(1+r) \cos \varphi \sin \theta)^{-3/2} \right) e_2. \end{aligned} \quad (4.15)$$

4.3.2 Replacing \mathbb{C} with \mathbb{H}

Conformal mappings rely entirely on complex numbers. By replacing the complex number $z = x + iy$ with a hypercomplex number $q = t + ix + jy + kz$ in ((4.1)), we get a mapping function defined by

$$w(q) = q + \frac{\lambda^2}{q}. \quad (4.16)$$

Here $w(q)$ is a transformed hypercomplex plane in \mathbb{H} . Since it is not feasible to map a four-dimensional geometry, a reduced quaternion $q = t + ix + jy$ is used instead. Thus the shapes can be plotted in three dimensions.

Note [12]: \mathbb{H} can be viewed as the Clifford algebra $Cl_{0,2}$. By setting $e_1 = i$, $e_2 = j$, a quaternion q can be read as follows:

$$q = x_0 + x_1 e_1 + x_2 e_2 + x_3 e_1 e_2.$$

The reduced quaternions

$$q = x_0 + x_1e_1 + x_2e_2$$

are the paravectors of $Cl_{0,2}$.

The main entity of our study is the newly formulated hypercomplex-valued function (4.16) which depends on a single reduced quaternion and the geometries obtained through this transformation. These are analyzed and explained in the following chapters.

Chapter 5

Euclidean Geometry

5.1 Introduction

In this chapter, the mapping function is subjected to an Euclidean sphere and the transformations are discussed.

Note: Euclidean geometry is deduced from the Euclid's postulates and these are mentioned in chapter 6.

5.2 Joukoswki profile - Euclidean

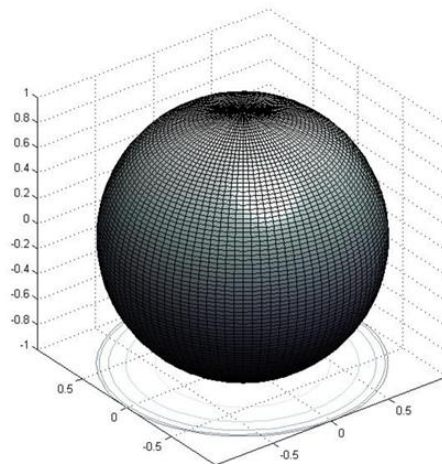


Figure 5.1: An Euclidean sphere

To begin with, consider the following parametrization of an Euclidean sphere

$$x_0 = r \sin \psi \cos \theta, \quad x_1 = r \sin \psi \sin \theta, \quad x_2 = r \cos \psi, \quad (5.1)$$

where $r > 0$ is the radius of the sphere, $0 \leq \psi \leq \pi$ and $0 \leq \theta \leq 2\pi$.

It is to be noted that $(x_0, x_1, x_2) \in \mathbb{R}^3$ represent the three components of a non-zero reduced quaternion. Therefore geometrically, we have a sphere or a ball of reduced quaternions.

The proposed Joukowski transformation in \mathbb{H} is

$$w(q) = q + \frac{\lambda^2}{q}. \quad (5.2)$$

Let us consider the polar decomposition of any quaternion [21]

$$q = re^{hv}, \quad (5.3)$$

where r and v are real with $r \geq 0$, and h is a pure unit quaternion. The expression (5.3) can also be written as

$$\begin{aligned} q &= re^{(ix+jy)v} \\ &= re^{ivx}e^{jvy} \\ &= r(\cos \alpha + i \sin \alpha)(\cos \beta + j \sin \beta), \end{aligned} \quad (5.4)$$

where $\alpha = vx$ and $\beta = vy$.

Now by setting the value of the transformation parameter λ equal to r and substituting q in (5.2) yields

$$\begin{aligned} w(q) &= r(\cos \alpha + i \sin \alpha)(\cos \beta + j \sin \beta) + r(\cos \alpha - i \sin \alpha)(\cos \beta - j \sin \beta) \\ &= r(\cos \alpha \cos \beta + j \cos \alpha \sin \beta + i \sin \alpha \cos \beta + k \sin \alpha \sin \beta) \\ &\quad + r(\cos \alpha \cos \beta - j \cos \alpha \sin \beta - i \sin \alpha \cos \beta + k \sin \alpha \sin \beta) \\ &= 2r(\cos \alpha \cos \beta + k \sin \alpha \sin \beta). \end{aligned} \quad (5.5)$$

In this case, the transformation causes the Euclidean sphere to map onto a *thin string*. This is seen in Figure 5.2. A closer look indicates that the geometry is ellipsoidal in shape along the x_0 axis.

For $\lambda < r$ and $\lambda > r$, the spheres are transformed to spheroids just as in Figure 5.3. The transformation is noticed to flow from a sphere to an oblate spheroid and then to a thin string. But, as soon as the value of λ is greater than r , it reverts back to an oblate spheroid and finally to a sphere.

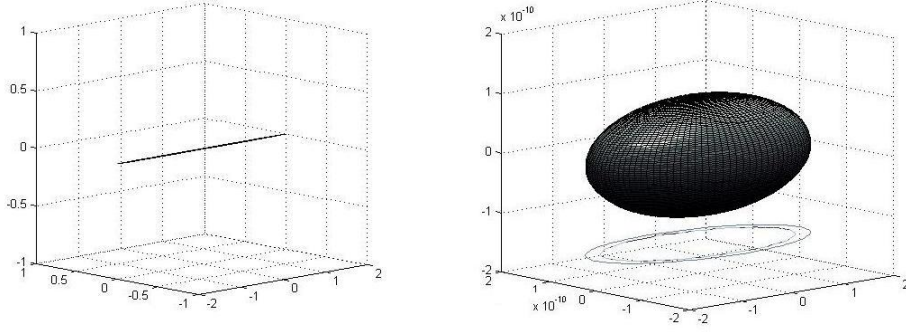


Figure 5.2: A thin string along x_0 axis. The limits of x_1 and x_2 axes (image on the right) are in $1e^{-10}$ s.

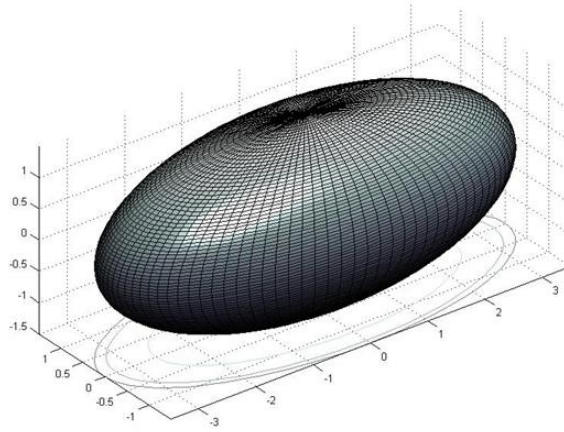


Figure 5.3: Ellipsoid

The transformation for $\lambda \neq r$ renders

$$\begin{aligned}
 w(q) &= r (\cos \alpha + i \sin \alpha)(\cos \beta + j \sin \beta) + \frac{\lambda^2}{r} (\cos \alpha - i \sin \alpha)(\cos \beta - j \sin \beta) \\
 &= \dots \\
 &= \left(r + \frac{\lambda^2}{r}\right) \cos \alpha \cos \beta + i \left(r - \frac{\lambda^2}{r}\right) \sin \alpha \cos \beta + j \left(r - \frac{\lambda^2}{r}\right) \cos \alpha \sin \beta \\
 &\quad + k \left(r + \frac{\lambda^2}{r}\right) \sin \alpha \sin \beta. \tag{5.6}
 \end{aligned}$$

If $x_0 = \left(r + \frac{\lambda^2}{r}\right) \cos \alpha \cos \beta$, $x_1 = \left(r - \frac{\lambda^2}{r}\right) \sin \alpha \cos \beta$, $x_2 = \left(r - \frac{\lambda^2}{r}\right) \cos \alpha \sin \beta$ and $x_3 = \left(r + \frac{\lambda^2}{r}\right) \sin \alpha \sin \beta$, then this can be written as,

$$\begin{aligned}
\frac{x_0^2}{\left(r + \frac{\lambda^2}{r}\right)^2} + \frac{x_1^2}{\left(r - \frac{\lambda^2}{r}\right)^2} + \frac{x_2^2}{\left(r - \frac{\lambda^2}{r}\right)^2} + \frac{x_3^2}{\left(r + \frac{\lambda^2}{r}\right)^2} \\
&= \cos^2 \alpha \cos^2 \beta + \sin^2 \alpha \cos^2 \beta \\
&\quad + \cos^2 \alpha \sin^2 \beta + \sin^2 \alpha \sin^2 \beta \\
&= \cos^2 \alpha (\cos^2 \beta + \sin^2 \beta) \\
&\quad + \sin^2 \alpha (\cos^2 \beta + \sin^2 \beta) \\
&= \cos^2 \alpha + \sin^2 \alpha = 1.
\end{aligned}$$

This is an equation of an ellipsoid in \mathbb{R}^4 with $a = \left(r + \frac{\lambda^2}{r}\right)$ as the equatorial radius and $b = \left(r - \frac{\lambda^2}{r}\right)$ as the polar radius.

Moreover it is to be noticed that just as in the 2-dimensional case of the Joukowski profile, the shape of an airfoil is obtained if the center of the sphere is slightly offset from the origin. The mapping function transforms the three dimensional spheres into suitable airfoils. Here again the desired transformation parameter λ is calculated using the equation

$$\lambda = r - |s|$$

where r is the radius and s is the co-ordinates of the center of the sphere.

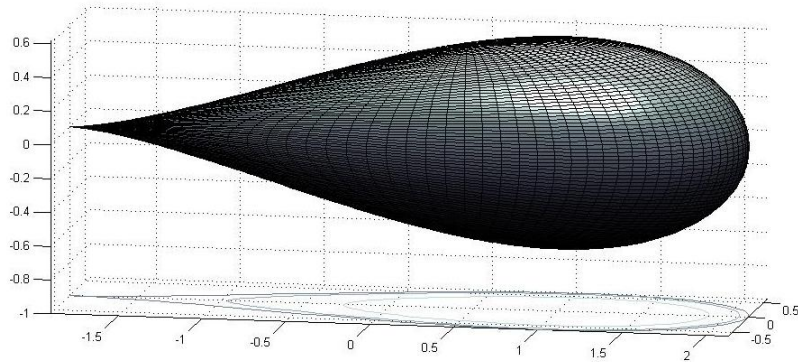


Figure 5.4: Symmetric airfoil in 3-dimension

A symmetric airfoil results if the center is offset on the x_0 axis. Besides if the center of the sphere is also moved parallel to the x_2 axis, a cambered non-symmetric airfoil is generated. The pictures of these airfoils are shown in Figure 5.4 and 5.5.

The transformation even caters for airfoils with negative camber as shown in Figure 5.6. This is observed if the center is moved along the negative x_2 axis.

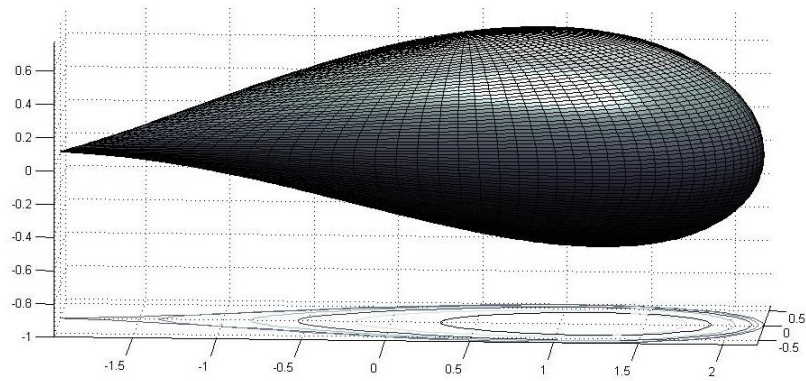


Figure 5.5: Cambered non-symmetric airfoil with positive camber

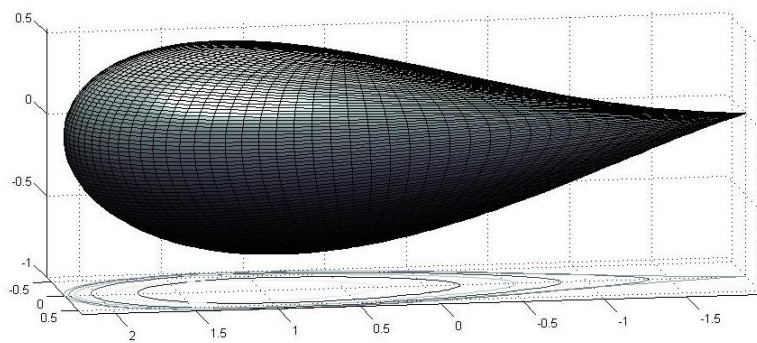


Figure 5.6: Cambered non-symmetric airfoil with negative camber

Chapter 6

Hyperbolic Geometry

6.1 Introduction

Hyperbolic geometry is a non-Euclidean geometry where the fifth axiom of the Euclid's postulates fails. The fifth axiom is also referred as the *parallel postulate* and it reads as follows:

For any given line l and a point P not on it, there is exactly one line through P that does not intersect l . As it can be imagined, on a hyperbolic plane or surface there are infinitely many different lines that pass through P and do not intersect l .

This can be visualized on the very few hyperbolic models that have been constructed so far. These models are designed within the Euclidean geometry that obeys the first four axioms of the Euclid's postulates:

1. *A straight line may be drawn from any point to any other point.*
2. *The straight line may be extended to any length.*
3. *A circle of any radius may be described around any point as a center.*
4. *Any two right angles are equal.*

The four commonly used models for the hyperbolic geometry are:

- The Upper half plane model
- The Unit ball model
- The Klein model and
- The hyperboloid model

These models are referred from [11] and are described below.

6.2 Hyperbolic models

6.2.1 Upper half space model

The Upper half space model includes the Euclidean upper half plane as its hyperbolic plane. It is traced out as follows :

$$\mathbb{R}_+^3 = \{(x, y, t) \in \mathbb{R}^3 : t > 0\}$$

with the hyperbolic metric induced by

$$ds^2 = \frac{dx^2 + dy^2 + dt^2}{t^2}, \quad l(\sigma) = \int_{\sigma} ds.$$

The geodesics are lines or portions of circles with their center on the boundary that they are orthogonal to the Euclidean plane. Here it is referred as an XY plane.

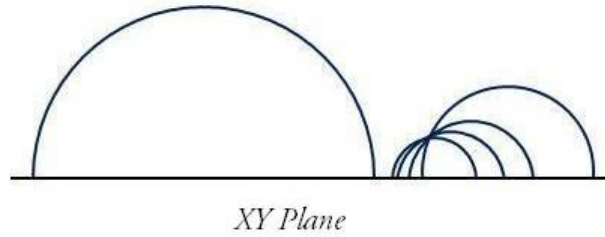


Figure 6.1: Upper half space model

The hyperbolic distance between any two points $P = (x, y, t)$ and $Q = (x', y', t')$ in the XY plane is given by

$$d_h(P, Q) = \operatorname{arcosh} \delta(P, Q), \quad (6.1)$$

where

$$\delta(P, Q) = \frac{(x - x')^2 + (y - y')^2 + t^2 + t'^2}{2tt'}. \quad (6.2)$$

The angles are the same as the Euclidean angles and tangents are drawn to the lines in order to calculate them.

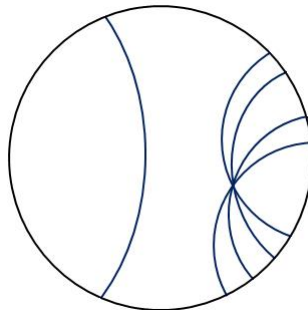


Figure 6.2: Unit ball model

6.2.2 Unit ball model

In the Unit ball model, the plane is the unit ball $B = \{x \in \mathbb{R}^3 \mid \|x\| < 1\}$ and the points are the Euclidean points. We consider the mapping

$$(x_1, x_2, x_3) \mapsto \left(\frac{2x_1}{x_1^2 + x_2^2 + (x_3 - 1)^2}, \frac{2x_2}{x_1^2 + x_2^2 + (x_3 - 1)^2}, \frac{1 - x_1^2 - x_2^2 - x_3^2}{x_1^2 + x_2^2 + (x_3 - 1)^2} \right)$$

from the unit ball to the upper half space \mathbb{R}_+^3 .

The hyperbolic metric in B is defined by

$$ds^2 = 4 \frac{dx_1^2 + dx_2^2 + dx_3^2}{1 - x_1^2 - x_2^2 - x_3^2}.$$

The geodesics are portions of circles or straight lines intersecting the boundary at right angles. As in the Upper half space model, the angles are the same as the Euclidean angles.

6.2.3 Klein model

In the Klein model, the plane is the unit ball (i.e.) the interior of the Euclidean unit sphere. The geodesics in this model are the straight line segments. Though this seems similar to the Euclidean space there are differences. The hyperbolic distance between any two points $P = (x, y, t)$ and $Q = (x', y', t')$ is given by

$$\operatorname{arcosh} \left(\frac{1 - xx' - yy' - tt'}{\sqrt{(1 - x^2 - y^2 - t^2)(1 - x'^2 - y'^2 - t'^2)}} \right). \quad (6.3)$$

The angles in this model are the same as the corresponding Euclidean angles.

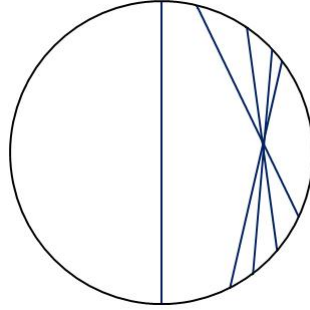
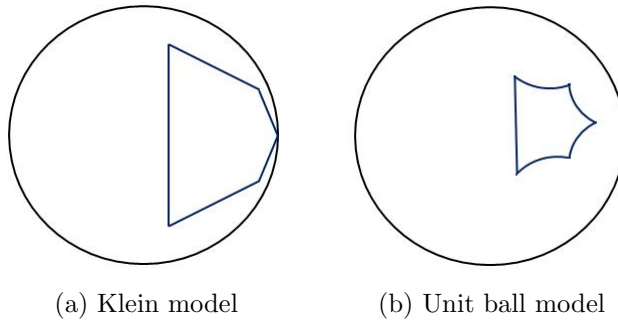
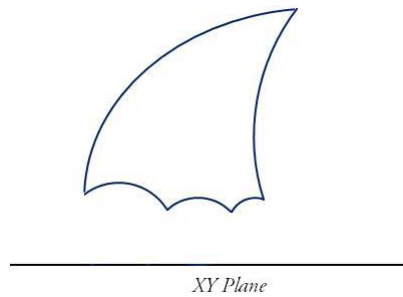


Figure 6.3: Klein model



(a) Klein model

(b) Unit ball model



(c) Upper half space model

Figure 6.4: An example of a regular pentagon in three hyperbolic models

6.2.4 Hyperboloid model

In the hyperboloid model, we consider the Minkowski metric in \mathbb{R}^4 . Let $x = (x_1, x_2, x_3, x_4)$.

$$\begin{aligned} \langle x, x \rangle &= x_4^2 - x_3^2 - x_2^2 - x_1^2 \\ \langle x, x \rangle = 0 &\iff x_4^2 = x_1^2 + x_2^2 + x_3^2 \\ \langle x, x \rangle = 1 &\iff x_4^2 - x_3^2 - x_2^2 - x_1^2 = 1. \end{aligned}$$

Let $x_4 > 0$. By restricting the Minkowski metric to the tangent planes of the hyperbola yields a positive definite quadratic form and this defines a Riemannian metric.

A hyperbola provided with this metric is the Hyperboloid model. This model is also referred as the *Lorentz model*.

6.3 Joukowski profile - Hyperbolic

In this section, we define a hyperbolic sphere in the Upper half space model and discuss the transformations obtained by implementing the hyperbolic ball in the mapping function as in the 3-dimensional Euclidean geometry.

Lemma 6.3.1 [11] *A hyperbolic sphere with a hyperbolic center $\zeta = \xi + i\eta + j\tau \in \mathbb{R}_+^3$ and hyperbolic radius r_h , i.e., the set of vectors*

$$\{z \in \mathbb{R}_+^3 \mid d_h(z, \zeta) = r_h\} \quad (6.4)$$

can also be defined as follows

$$\left\{ z \in \mathbb{R}_+^3 \mid \frac{|z - \zeta|}{|z - \hat{\zeta}|} = \tanh\left(\frac{r_h}{2}\right) \right\}, \quad (6.5)$$

where $\hat{\zeta} = \xi + i\eta - j\tau$.

Proof. We recall that the hyperbolic distance in the Upper half space model is $d_h(z, \zeta) = \text{arcosh } \delta(z, \zeta)$ where

$$\delta(z, \zeta) = \frac{(x - \xi)^2 + (y - \eta)^2 + t^2 + \tau^2}{2t\tau}.$$

Consequently,

$$d_h(z, \zeta) = r_h \iff \delta(z, \zeta) = \cosh r_h = v$$

and

$$(x - \xi)^2 + (y - \eta)^2 + t^2 + \tau^2 = v2t\tau. \quad (*)$$

Therefore

$$\begin{aligned} |z - \zeta|^2 &= (x - \xi)^2 + (y - \eta)^2 + (t - \tau)^2 \\ &= v2t\tau - 2t\tau \\ &= (v - 1)2t\tau. \end{aligned}$$

$$\begin{aligned} |z - \hat{\zeta}|^2 &= (x - \xi)^2 + (y - \eta)^2 + (t + \tau)^2 \\ &= v2t\tau + 2t\tau \\ &= (v + 1)2t\tau. \end{aligned}$$

$$\implies \frac{|z - \zeta|^2}{|z - \hat{\zeta}|^2} = \frac{v - 1}{v + 1} = \frac{\cosh r_h - 1}{\cosh r_h + 1} = \tanh^2 \left(\frac{r_h}{2} \right). \quad (6.6)$$

We also notice that from (*)

$$\begin{aligned} (x - \xi)^2 + (y - \eta)^2 + \underbrace{t^2 - 2vt\tau + v^2\tau^2}_{(t-v\tau)^2} &= \lambda^2\tau^2 - \tau^2 \\ &= (\lambda^2 - 1)\tau^2 \\ &= (\cosh^2 r_h - 1)\tau^2 \end{aligned}$$

By using the basic trigonometric identity $\cosh^2 r_h - 1 = \sinh^2 r_h$, we have

$$\begin{aligned} (x - \xi)^2 + (y - \eta)^2 + (t - \tau \cosh r_h)^2 &= (\sinh^2 r_h)\tau^2 \\ &= \tau^2 \sinh^2 r_h. \end{aligned}$$

Thus summing up, a non-Euclidean sphere with non-Euclidean center ζ and non-Euclidean radius r_h is an Euclidean sphere with the Euclidean center

$$\hat{\zeta} = \xi + i\eta + j\tau \cosh r_h \quad (6.7)$$

and Euclidean radius

$$r = \tau \sinh r_h. \quad (6.8)$$

Let us consider the following spherical co-ordinates of a hyperbolic sphere.

$$y_0 = r \sin \psi \cos \theta + \xi, \quad y_1 = r \sin \psi \sin \theta + \eta, \quad y_2 = r \cos \psi + \tau \cosh r_h, \quad (6.9)$$

where r is the Euclidean radius of the hyperbolic sphere, r_h is the hyperbolic radius, $0 \leq \psi \leq \pi$ and $0 \leq \theta \leq 2\pi$. The co-ordinates $(y_0, y_1, y_2) \in \mathbb{R}^3$ represent the three components of a non-zero reduced quaternion of the form $y_0 + iy_1 + jy_2$. Since *Poincaré upper half space* is a Riemannian manifold (\mathbb{R}_+^3, g_1) with the metric

$$g_1 = \frac{dy_0^2 + dy_1^2 + dy_2^2}{y_2^2}, \quad (6.10)$$

and

$$\mathbb{R}_+^3 = \{(y_0, y_1, y_2) \in \mathbb{R}^3 : y_2 > 0\}$$

the third component $y_2 > 0$.

The revised Joukowski transformation is given by

$$w(q) = \left(q - \hat{\zeta} \right) + \frac{\lambda^2}{\left(q - \hat{\zeta} \right)}, \quad (6.11)$$

where $\hat{\zeta}$ is the center of the hyperbolic sphere.

Now by subjecting the sphere into the map yields similar cross-sectional shapes as in the Euclidean cases. It is to be noticed as the value of y_2 is increased the hyperbolic distance between the points on the boundary and center of the sphere decreases and vice versa. This is anticipated because if $k > 0$ in (6.10) then a geometry which is similar to that of a hyperbolic space is generated and distances decrease as y_2 increases and vice versa [18].

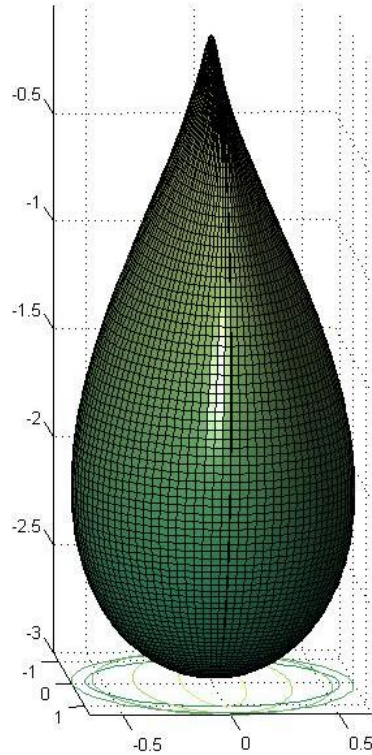


Figure 6.5: A symmetric airfoil

Note [18]: In the expression (6.10)

- *If $k = 0$, Euclidean geometry is obtained.*
- *If $k < 0$, we obtain a geometry with ‘infinte distances’ as $y_2 \rightarrow \infty$. But distances ‘tend to zero’ in the neighbourhood of y_2 .*

The transformation function generates spheres by preserving the center of the hyperbolic sphere closer to the origin and increasing the Euclidean radius gradually.

Airfoils are visualized at certain locations of the hyperbolic sphere. A symmetric airfoil is generated if the center of the sphere is moved parallel to the y_2 axis. However if the center is also moved parallel to the y_1 axis, the airfoil gets tilted and its thickness

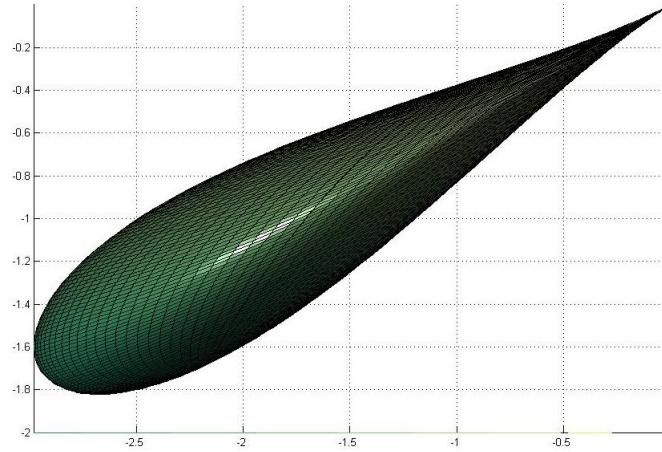


Figure 6.6: View of a symmetric airfoil tilted to an angle along Y and Z axes

- maximum distance between the upper and lower surface of the airfoil - gets reduced (Figure 6.6).

Similar airfoil shapes are obtained if the center of the hyperbolic sphere is offset *just* on the y_1 axis. Certainly, the y_2 co-ordinate takes the smallest positive real number here and it remains unmoved. As a result there is no change in the radius of the hyperbolic sphere. The parameter λ is calculated as follows for the above transformations:

$$\lambda = r - |s|$$

where r is the Euclidean radius of the hyperbolic sphere and s is the hyperbolic center.

However if λ is set equal to the Euclidean radius r and if the center is offset on the y_2 axis a non-cambered symmetric airfoil is generated anew.

6.4 Non-Euclidean center in a hyperbolic sphere

Undeniably it would be of interest to know where exactly the hyperbolic center is with respect to the Euclidean and hyperbolic spheres and how it moves as y_2 is varied.

Lemma 6.4.1 *The hyperbolic sphere centered at*

$$\hat{\zeta} = \xi + i\eta + j\tau \cosh r_h,$$

lies above the Euclidean center and the hyperbolic center is inside the Euclidean sphere.

Proof. The distance

$$\begin{aligned} |\tau e_n - \tau e_n \cosh r_h| &= |\tau - \tau \cosh r_h| \\ &= \tau \cosh r_h - \tau. \end{aligned} \tag{6.12}$$

We show that (6.12) is less than the Euclidean radius. Indeed

$$\begin{aligned}
 & \tau(\cosh r_h - 1) < \tau \sinh r_h \\
 \Leftrightarrow & \frac{e^{r_h} + e^{-r_h}}{2} - 1 < \frac{e^{r_h} - e^{-r_h}}{2} \\
 \Leftrightarrow & e^{r_h} + e^{-r_h} - 2 < e^{r_h} - e^{-r_h} \\
 & \Leftrightarrow 2e^{-r_h} < 2 \\
 & \Leftrightarrow e^{-r_h} < 1.
 \end{aligned}$$

This is true for $r_h > 0$.

To illustrate the above lemma, a hyperbolic and an Euclidean sphere are sketched with their respective centers.

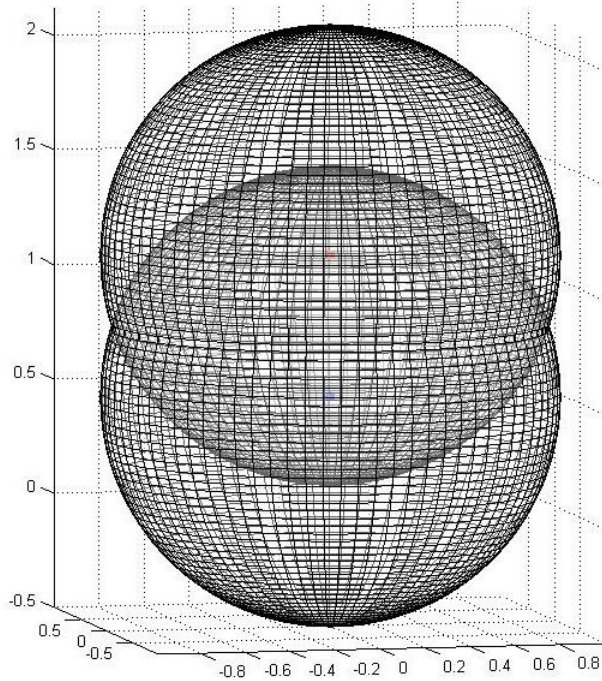


Figure 6.7: The hyperbolic sphere lies with its lower half inside the Euclidean sphere. The Non-Euclidean center (red) is located in the Euclidean sphere and above the Euclidean center (blue).

The hyperbolic center defined by

$$\hat{\zeta} = \xi + i\eta + j\tau \cosh r_h,$$

is located above the Euclidean center and inside the Euclidean sphere as in Figure 6.7. The lower half of the hyperbolic sphere is submerged inside the Euclidean sphere. We

recall that the radius of a hyperbolic sphere decreases as the value of y_2 is increased and vice versa [18]. This is a particular case of the *Poincare Upper half-space model* and is less surprising.

As y_2 is increased, the hyperbolic sphere moves into the Euclidean sphere. As a result the hyperbolic center is seen closer to the Euclidean center. This is plotted in Figure 6.8.

However, by fixing y_2 and increasing the Euclidean radius the hyperbolic radius increases and the hyperbolic center moves further away from the Euclidean center but rather remains within the premises of the Euclidean sphere. Thus, in both the cases, the hyperbolic center is located inside and above the Euclidean center in the Euclidean sphere as expected.

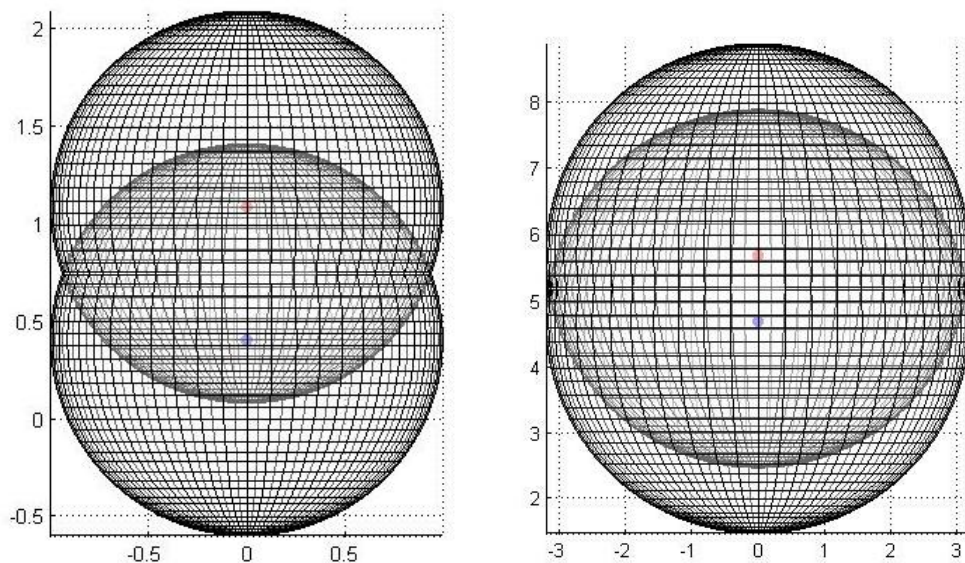


Figure 6.8: The hyperbolic sphere moves into the Euclidean sphere as the y_2 co-ordinate is increased.

Chapter 7

Generalities

In this chapter, we review the generalized function theory for the mapping $f : \Omega \subset \mathbb{R}^3 \rightarrow \mathbb{H}$ and it is referred from [6] and [12].

7.1 Hypermonogenic

7.1.1 M.Riesz system in \mathbb{R}^3

Let us recall the Cauchy-Riemann equations that characterizes the holomorphic functions $f = u + iv$

$$\left. \begin{array}{l} \frac{\partial u}{\partial x} = \frac{\partial v}{\partial y}, \\ \frac{\partial u}{\partial y} = -\frac{\partial v}{\partial x} \end{array} \right\} \iff \frac{\partial f}{\partial x} + i \frac{\partial f}{\partial y} = 0 \quad \left(= 2 \frac{\partial f}{\partial \bar{z}} \right)$$

It is remarked that these equations naturally extend to \mathbb{R}^3 . That is to say, for the mapping $f : \Omega \subset \mathbb{R}^3 \rightarrow \mathbb{H}$, Ω is an open subset in \mathbb{R}^3 , the following operators are introduced.

$$D_l f = \frac{\partial f}{\partial x} + i \frac{\partial f}{\partial y} + j \frac{\partial f}{\partial t}, \quad (7.1)$$

$$D_r f = \frac{\partial f}{\partial x} + \frac{\partial f}{\partial y} i + \frac{\partial f}{\partial t} j. \quad (7.2)$$

The above operators are also called as the *Dirac operators*. Moreover, we have

$$D_l f = 0, \quad (\text{respectively } D_r f = 0).$$

The solutions $f : \Omega \rightarrow Cl_{0,n}$, ($\Omega \subset \mathbb{R}^{n+1}$ open) of the above equations are called *left(right) monogenic* functions.

For functions $f = u + iv + jw : \Omega \subset \mathbb{R}^3 \longrightarrow \mathbb{R}^3$, the preceding equations are equivalent and lead to the following system:

$$\left. \begin{aligned} \frac{\partial u}{\partial x} - \frac{\partial v}{\partial y} - \frac{\partial w}{\partial t} &= 0, \\ \frac{\partial u}{\partial y} &= -\frac{\partial v}{\partial x}, \quad \frac{\partial u}{\partial t} = -\frac{\partial w}{\partial x}, \quad \frac{\partial v}{\partial t} = \frac{\partial w}{\partial y} \end{aligned} \right\} (R)$$

It is referred as *M.Riesz system*.

By replacing f by $g = \bar{f}$, the system (R) is read as follows [12]:

$$\operatorname{div} g = 0 \tag{7.3}$$

$$\operatorname{rot} g = 0. \tag{7.4}$$

From (7.4), it is concluded that solutions of (R) are locally of the form

$$f = \frac{\partial h}{\partial x} - i \frac{\partial h}{\partial y} - j \frac{\partial h}{\partial t}.$$

Besides, by considering (7.3) the function h defined on some open set $\Omega \subset \mathbb{R}^3$ is *harmonic*, i.e. it satisfies the Laplace equation $\Delta h = 0$.

Remark: The components u , v and w of an (R)-solution are all harmonic.

Definition 7.1.1 Let $\Omega \subset \mathbb{R}^{n+1}$ be open. A continuously differentiable function $f : \Omega \longrightarrow Cl_{0,n}$ is called (left) hypermonogenic, if $M_n f(x) = 0$ for any $x \in \Omega \setminus \{x \mid x_n = 0\}$. M_n is the modified Dirac-Fueter operator which is defined as follows: For any $f : \Omega \setminus \{x \mid x_n = 0\} \longrightarrow Cl_{0,n}$, $\Omega \subset \mathbb{R}^{n+1}$ is open,

$$M_n f(x) = D_l f(x) + \frac{n-1}{x_n} (Q_{n-1} f)'(x).$$

7.1.2 Modified system in \mathbb{R}^3

The power of a reduced quaternion $q = x + iy + jt$ is also a reduced quaternion. This is noticed from the polar form of q . If $q = r(\cos \varphi + i \sin \varphi + j \sin \varphi \sin \theta)$ where $r = |q|$ and φ and θ are Euler angles, then

$$q^n = r^n (\cos(n\varphi) + i \sin(n\varphi) + j \sin(n\varphi) \sin \theta). \tag{7.5}$$

This is a generalization of De Moivre's identity.

In otherwords, $q \longrightarrow q^n$ maps \mathbb{R}^3 onto itself. But this mapping does not solve the (R)-system and we have $D_l f = 1 + i^2 + j^2 = -1 \neq 0$. Therefore, the M.Riesz system is modified as follows:

- (i) The Euclidean metric i.e. $ds^2 = dx^2 + dy^2 + dt^2$ is replaced with the hyperbolic metric

$$ds^2 = \frac{dx^2 + dy^2 + dt^2}{t^2} \quad (t > 0).$$

- (ii) The function $f = u + iv + jw$ satisfies the *modified system* below.

$$\left. \begin{aligned} t \left(\frac{\partial u}{\partial x} - \frac{\partial v}{\partial y} - \frac{\partial w}{\partial t} \right) + w &= 0 \\ \frac{\partial u}{\partial y} = -\frac{\partial v}{\partial x}, \quad \frac{\partial u}{\partial t} = -\frac{\partial w}{\partial x}, \quad \frac{\partial v}{\partial t} = \frac{\partial w}{\partial y} \end{aligned} \right\} (H)$$

The solutions $f : \Omega \subset \mathbb{R}^3 \rightarrow \mathbb{H}$ of (H) are called (H)-solutions and are well defined on any open set $\Omega \subset \mathbb{R}^3$ (not just on the open subsets of the Upper half space \mathbb{R}_+^3). Every (H)-solution can be atleast locally represented as

$$f = \frac{\partial H}{\partial x} - i \frac{\partial H}{\partial y} - j \frac{\partial H}{\partial t}.$$

H is *hyperbolic harmonic*, i.e. it satisfies the *Laplace-Beltrami* equation associated with the hyperbolic metric.

$$t\Delta H - \frac{\partial H}{\partial t} = 0 \quad (\Delta = \frac{\partial^2}{\partial x^2} + \frac{\partial^2}{\partial y^2} + \frac{\partial^2}{\partial t^2}). \quad (*)$$

Remark: If $f = u + iv + jw$ is an (H)-solution, the components u and v are hyperbolic harmonic. However, the third component w satisfies the following equation:

$$t^2\Delta H - t\frac{\partial H}{\partial t} + H = 0. \quad (**)$$

Both the equations (*) and (**) are eigen functions of the Laplace-Beltrami operator Δ_{LB} associated with the above metric:

$$\Delta_{LB} = t^2 \left(\Delta - \frac{1}{t} \frac{\partial}{\partial t} \right).$$

Example of (*).

Consider $H(z) = \log |z|$, the fundamental solution of (*) with respect to 0. Then

$$\begin{aligned} f(z) &= \overline{\text{grad}}(\log |z|) \\ &= \left(\frac{\partial}{\partial x} - i \frac{\partial}{\partial y} - j \frac{\partial}{\partial t} \right) (\log |z|) \end{aligned}$$

We have $\log |z| = \log |x + iy + jt| = \log(x^2 + y^2 + t^2)^{1/2}$ and therefore

$$\begin{aligned} f(z) &= \frac{x}{x^2 + y^2 + t^2} - i \frac{y}{x^2 + y^2 + t^2} - j \frac{t}{x^2 + y^2 + t^2} \\ &= \frac{x - iy - jt}{x^2 + y^2 + t^2} \\ &= \frac{\bar{z}}{|z|^2} \\ &= \frac{\bar{z}}{z\bar{z}} \\ &= z^{-1} \end{aligned}$$

is an (H) -solution. Notice that since f is an (H) -solution, so are the partial derivatives

$$\frac{\partial f}{\partial x}, \frac{\partial f}{\partial y}.$$

With $z \mapsto z^{-1}$, it follows that the mapping $z \mapsto z^{-n}$ ($n \in \mathbb{N}$) is an (H) -solution. This is because the following relation holds:

$$\frac{\partial^n (z^{-1})}{\partial x^n} = (-1)^n n! z^{-(n+1)}. \quad (7.6)$$

We prove the above result by induction.

Let us consider the case $n = 1$ in equation (7.6) and note that the derivative of a product of two functions is given by

$$\frac{\partial}{\partial x}(fg) = \frac{\partial f}{\partial x}g + f\frac{\partial g}{\partial x}.$$

Hence

$$0 = \frac{\partial}{\partial x}(zz^{-1}) = \frac{\partial z}{\partial x}z^{-1} + z\frac{\partial z^{-1}}{\partial x} = z^{-1} + z\frac{\partial z^{-1}}{\partial x},$$

which implies

$$\frac{\partial z^{-1}}{\partial x} = (-1)z^{-2}.$$

Let us assume the statement is true for any positive integer k , that is,

$$\frac{\partial}{\partial x}(z^{-k}) = (-k)z^{-(k+1)}.$$

Consequently, we have

$$(-k)z^{-(k+1)} = \frac{\partial}{\partial x}(z^{-(k+1)}z) = \frac{\partial z^{-(k+1)}}{\partial x}z + z^{-(k+1)}\frac{\partial z}{\partial x} = \frac{\partial z^{-(k+1)}}{\partial x}z + z^{-(k+1)}.$$

Therefore, it is inferred that

$$\frac{\partial}{\partial x}(z^{-(k+1)}) = (-1)(k+1)z^{-(k+1)}z^{-1} = (-1)(k+1)z^{-(k+2)}.$$

Thus by the principle of mathematical induction, the statement is true for all $k \in \mathbb{N}$.

Since the equation also holds for $n = 2$, that is,

$$\frac{\partial^2}{\partial x^2}(z^{-1}) = -\frac{\partial}{\partial x}(z^{-2}) = 2z^{-3},$$

we claim that

$$\frac{\partial^n}{\partial x^n}(z^{-1}) = (-1)^n n! z^{-(n+1)}.$$

Assume that the equation holds for $n = k$. Then,

$$\frac{\partial^k}{\partial x^k}(z^{-1}) = (-1)^k k! z^{-(k+1)}.$$

As a result, we deduce

$$\begin{aligned} \frac{\partial^{k+1}}{\partial x^{k+1}}(z^{-1}) &= (-1)^k k! \frac{\partial}{\partial x}(z^{-(k+1)}) \\ &= (-1)^k k! (-1)(k+1)z^{-(k+2)} \\ &= (-1)^{k+1} (k+1)! z^{-(k+2)}. \end{aligned}$$

By the principle of mathematical induction, the statement is true for all positive integers $n \in \mathbb{N}$. Hence z^{-n} is an (H) -solution for all $n \in \mathbb{N}$.

Preliminaries

The involution $' : \mathbb{H} \longrightarrow \mathbb{H}$ is an isomorphism defined by

$$q' = x_0 - x_1 e_1 - x_2 e_2 + x_{12} e_{12}$$

where $x_0, x_1, x_2, x_{12} \in \mathbb{R}$.

Some properties of involution are:

$$z e_2 = e_2 z' = e_2 \bar{z}, \quad z \in \mathbb{C}, \quad (7.7)$$

$$q' e_2 = e_2 \hat{q}, \quad q \in \mathbb{H}. \quad (7.8)$$

where $\hat{q} = x_0 + x_1 e_1 - x_2 e_2 - x_{12} e_{12}$.

Let $P : \mathbb{H} \longrightarrow \mathbb{C}$ and $Q : \mathbb{H} \longrightarrow \mathbb{C}$ be the projecting operators defined by

$$P(z_0 + z_1 e_2) = z_0,$$

$$Q(z_0 + z_1 e_2) = z_1.$$

Note that for any $x \in \mathbb{H}$

$$\begin{aligned} P^2x &= Px, \\ Q^2x &= 0, \\ P(Qx) &= Qx, \\ Q(Px) &= 0. \end{aligned}$$

Lemma 7.1.2 *If $a, b \in \mathbb{H}$, then*

$$\begin{aligned} P(ab) &= PaPb - Qa(Qb)', \\ Q(ab) &= qQb + (Qa)b', \\ P(a') &= (Pa)', \\ Q(a') &= -(Qa)'. \end{aligned}$$

Lemma 7.1.3 *If $w \in \mathbb{H}$ then*

$$\begin{aligned} Qw &= \frac{e_2w' - we_2}{2}, \\ Pw &= -\frac{we_2 + e_2w'}{2}e_2. \end{aligned}$$

The *modified Dirac operator* is defined by

$$(M_k f)(x) = (Df)(x) + \frac{k}{x_2} Q' f \quad (7.9)$$

where D is the operator defined in (7.1). The operator \bar{M} is given by

$$(\bar{M}_k f)(x) = (\bar{D}f)(x) - \frac{k}{x_2} Q' f. \quad (7.10)$$

Now we have

$$M_k f + \bar{M}_k f = Df + \bar{D}f = 2 \frac{\partial f}{\partial x_0}.$$

Definition 7.1.4 *Let Ω be an open subset of \mathbb{R}^3 . If $f \in C^2(\Omega)$ and $M_k f(x) = 0$ for any $x \in \Omega \setminus \{x \mid x_2 = 0\}$ then the function f is called k -hypermonogenic in Ω . If f is paravector valued k -hypermonogenic in Ω , then f is called an H_k -solution. If a function is 1-hypermonogenic, then it is just referred as hypermonogenic.*

Lemma 7.1.5 *Let Ω be an open subset of \mathbb{R}^3 . If the components of a function $f : \Omega \rightarrow \mathbb{H}$ are partially differentiable, then*

$$P(Df) = D_1(Pf) - \frac{\partial(Qf)'}{\partial x_2} \quad (7.11)$$

$$Q(Df) = D_1(Qf) + \frac{\partial(Pf)'}{\partial x_2}, \quad (7.12)$$

where

$$D_1f = \frac{\partial f}{\partial x_0} + e_1 \frac{\partial f}{\partial x_1}.$$

Proof. Let us decompose, $f = Pf + (Qf)e_2$. Now

$$\begin{aligned} Df &= D(Pf) + D((Qf)e_2) \\ &= \frac{\partial(Pf)}{\partial x_0} + e_1 \frac{\partial(Pf)}{\partial x_1} + e_2 \frac{\partial(Pf)}{\partial x_2} + \frac{\partial((Qf)e_2)}{\partial x_0} + e_1 \frac{\partial((Qf)e_2)}{\partial x_1} + e_2 \frac{\partial((Qf)e_2)}{\partial x_2} \\ &= D_1(Pf) + e_2 \frac{\partial(Pf)}{\partial x_2} + D_1((Qf)e_2) - \frac{\partial(Qf)'}{\partial x_2} \quad \text{using (7.7)} \\ &= D_1(Pf) - \frac{\partial(Qf)'}{\partial x_2} + \left(D_1(Qf) + \frac{\partial(Pf)'}{\partial x_2} \right) e_2. \end{aligned}$$

Lemma 7.1.6 *Let $f : \Omega \rightarrow \mathbb{H}$ be twice continuously differentiable on an open subset $\Omega \subset \mathbb{R}^3$. Then*

$$\begin{aligned} \bar{M}_k M_k f &= M_k \bar{M}_k f \\ &= \Delta(Pf) - \frac{k}{x_2} \frac{\partial Pf}{\partial x_2} + \left(\Delta(Qf) - \frac{k}{x_2} \frac{\partial Qf}{\partial x_2} + \frac{k}{x_2^2} Qf \right) e_2 \\ &= \Delta f - k \frac{\partial f}{x_2 \partial x_2} + k \frac{e_2 f' e_2 + f}{2x_2^2}, \end{aligned}$$

where Δ is the Laplacian in \mathbb{R}^3 .

By the preceding lemma 7.1.5,

$$\begin{aligned} QM_k f &= Q(Df) + \frac{k}{x_2} Q(Q'f) \\ &= D_1(Qf) + \frac{\partial(P'f)}{\partial x_2}. \end{aligned}$$

We calculate

$$\begin{aligned} \bar{M}_k M_k f &= \bar{D}Df + k \left(\bar{D} \left(\frac{Q'f}{x_2} \right) - D \left(\frac{Q'f}{x_2} \right) \right) - \left(\frac{k}{x_2} Q'f \right)^2 \\ &= \bar{D}Df + k \bar{D} \left(\frac{Q'f}{x_2} \right) - k Q' \left(\frac{Df}{x_2} \right) \\ &= \bar{D}Df + k \bar{D} \left(\frac{Q'f}{x_2} \right) - \frac{k}{x_2} \left((D_1 Qf)' + \frac{\partial Pf}{\partial x_2} \right) \end{aligned}$$

Since

$$\begin{aligned}\bar{D}\left(\frac{Q'f}{x_2}\right) &= \frac{\partial\left(\frac{Q'f}{x_2}\right)}{\partial x_0} - e_1\frac{\partial\left(\frac{Q'f}{x_2}\right)}{\partial x_1} - e_2\frac{\partial\left(\frac{Q'f}{x_2}\right)}{\partial x_2} \\ &= \frac{1}{x_2}\frac{\partial Q'f}{\partial x_0} - \frac{1}{x_2}\sum_{i=1}^2 e_i\frac{\partial Q'f}{\partial x_i} + e_2\frac{Q'f}{x_2^2} \\ &= \frac{(D_2Qf)'}{x_2} + \frac{Qf}{x_2^2}e_2 - \frac{1}{x_2}\frac{\partial Qf}{\partial x_2}e_2,\end{aligned}$$

we obtain

$$\begin{aligned}\bar{M}_k M_k f &= \bar{D}Df + k\left(\frac{(D_2Qf)'}{x_2} + \frac{Qf}{x_2^2}e_2 - \frac{1}{x_2}\frac{\partial Qf}{\partial x_2}e_2\right) - \frac{k}{x_2}\left((D_1Qf)' + \frac{\partial Pf}{\partial x_2}\right) \\ &= \Delta Pf - \frac{k}{x_2}\frac{\partial Pf}{\partial x_2} + \left(\Delta Qf - \frac{k}{x_2}\frac{\partial Qf}{\partial x_2} + k\frac{Qf}{x_2^2}\right)e_2.\end{aligned}$$

Thus we have

$$M_k \bar{M}_k f = \Delta f - k\frac{\partial f}{x_2 \partial x_2} + k\frac{Qf e_2}{x_2^2}. \quad (7.13)$$

By lemma 7.1.3 it is deduced that

$$M_k \bar{M}_k f = \Delta f - k\frac{\partial f}{x_2 \partial x_2} + k\frac{e_2 f' e_2 + f}{2x_2^2}.$$

Note that from the definitions $M_k + \bar{M}_k = 2\frac{\partial f}{\partial x_0}$.

$$\begin{aligned}M_k^2 f + M_k \bar{M}_k f &= 2M_k\left(\frac{\partial f}{\partial x_0}\right) \\ &= 2\frac{\partial M_k f}{\partial x_0} \\ &= (M_k + \bar{M}_k)(M_k f) \\ &= M_k^2 f + \bar{M}_k M_k f.\end{aligned}$$

which implies that $M_k \bar{M}_k f = \bar{M}_k M_k f$.

Definition 7.1.7 Let $f : \Omega \rightarrow \mathbb{H}$ be twice continuously differentiable on an open subset $\Omega \subset \mathbb{R}^3$. If $\bar{M}_k M_k f = 0$ for any $x_2 \neq 0$, then f is called k -hyperbolic harmonic. If f is 1-hyperbolic harmonic, then f is called hyperbolic harmonic.

Corollary 7.1.8 Let $f : \Omega \rightarrow \mathbb{H}$ be a k -hypermonogenic function $\Omega \subset \mathbb{R}^3$, then f is real analytic.

Proposition 7.1.9 The function x^m is hypermonogenic for all $m \in \mathbb{Z}$.

Lemma 7.1.10 *An element $x \in \mathbb{H}$ is a paravector if and only if*

$$\sum_{i=0}^2 e_i x e_i = -x'.$$

Theorem 7.1.11 *Let Ω be an open subset of \mathbb{R}^3 and $f : \Omega \rightarrow \mathbb{H}$ be hypermonogenic. The product $f(x)x$ is hypermonogenic if and only if f is an H-solution.*

Proof. Let us assume that $f : \Omega \rightarrow \mathbb{H}$ and $f(x)x$ are hypermonogenic. Then

$$\begin{aligned} M_1(fx) &= (Dfx) + \frac{Q'(fx)}{x_2} \\ &= \left(Df + \frac{Q'f}{x_2} \right) x + f' + \sum_{i=0}^2 e_i f e_i \\ &= (M_1 f) x + f' + \sum_{i=0}^2 e_i f e_i \end{aligned}$$

Since we assume that f and $f(x)x$ are monogenic (i.e). $M_1(fx) = 0$, $M_1 f = 0$. Therefore

$$0 = M_1(fx) = f' + \sum_{i=0}^2 e_i f e_i.$$

By lemma 7.1.10 f is paravector valued and by definition f is an H-solution. The converse can be proved similarly.

Theorem 7.1.12 *Let Ω be an open subset of \mathbb{R}^3 and $F : \Omega \rightarrow \mathbb{H}$ be hypermonogenic. The product $f(x) = F(x)x^{-1}$ is hypermonogenic in $\Omega \setminus \{0\}$ if and only if it is paravector valued.*

Proof. Let us assume that $F : \Omega \rightarrow \mathbb{H}$ and $f(x) = F(x)x^{-1}$ are hypermonogenic. Since $F(x) = (F(x)x^{-1})x$, from theorem 7.1.11 $(F(x)x^{-1})$ is paravector valued.

Conversely, assume that f is paravector valued and F is hypermonogenic. Then by lemma 7.1.10,

$$\begin{aligned} 0 = M_1 F &= D(F) + \frac{Q'(F)}{x_2} \\ &= D(fx) + \frac{Q'(fx)}{x_2} \\ &= \left(Df + \frac{Q'f}{x_2} \right) x + f' + \sum_{j=0}^2 e_j f e_j \\ &= (M_1 f) x + f' + \sum_{j=0}^2 e_j f e_j \\ &= (M_1 f) x. \end{aligned}$$

Therefore f is hypermonogenic.

Corollary 7.1.13 *The function x^{-m} is an H -solution.*

Lemma 7.1.14 *Let Ω be an open subset of \mathbb{R}^3 and $f : \Omega \rightarrow \mathbb{H}$ be k -hypermonogenic. Then $\frac{\partial f}{\partial x_l}$ is hypermonogenic for $l=0,1$.*

Proposition 7.1.15 *Let Ω be an open subset of \mathbb{R}^3 and $f : \Omega \rightarrow \mathbb{H}$ be 1-hypermonogenic. Then f is monogenic on $\Omega \cap \mathbb{C}$.*

Theorem 7.1.16 *Let Ω be an open subset of \mathbb{R}^3 and $f : \Omega \rightarrow \mathbb{H}$ be a mapping with continuous partial derivatives. Then the equation $M_k f = 0$ is equivalent with the system of equations*

$$D_1(Pf) - \frac{\partial Q'f}{\partial x_2} + k \frac{Q'f}{x_2} = 0, \quad (7.14)$$

$$D_1(Qf) + \frac{\partial P'f}{\partial x_2} = 0, \quad (7.15)$$

where $D_1 = \sum_{i=0}^1 e_i \frac{\partial f}{\partial x_i}$.

The corresponding system for monogenic functions is the following.

Theorem 7.1.17 *Let Ω be an open subset of \mathbb{R}^3 and $f : \Omega \rightarrow \mathbb{H}$ be a mapping with continuous partial derivatives. Then the equation $Df = 0$ is equivalent with the system of equations*

$$D_1(Pf) - \frac{\partial Q'f}{\partial x_2} = 0, \quad (7.16)$$

$$D_1(Qf) + \frac{\partial P'f}{\partial x_2} = 0. \quad (7.17)$$

Proposition 7.1.18 *Let Ω be an open subset of \mathbb{R}^3 . If $f : \Omega \rightarrow \mathbb{H}$ is an H_k -solution, then*

$$\frac{\partial f}{\partial x_0} = \bar{D}(Re f) \quad (7.18)$$

Lemma 7.1.19 *If $f : \Omega \rightarrow \mathbb{H}$ is twice continuously differentiable, then*

$$\Delta(xf) = 2Df + x\Delta f.$$

Lemma 7.1.20 *If $f : \Omega \rightarrow \mathbb{H}$ is twice continuously differentiable, then*

$$M_k \bar{M}_k(xf) = 2M_k f + xM_k \bar{M}_k f.$$

Proof. From lemma 7.1.6, we have

$$M_k \bar{M}_k(xf) = \Delta(xf) - k \frac{\partial(xf)}{x_2 \partial x_2} + k \frac{Q(xf)e_2}{x_2^2}.$$

The product rule of Q leads to

$$Q(xf) = xQf + x_2f'.$$

Applying the lemma 7.1.19, we obtain

$$\begin{aligned} M_k \bar{M}_k f(x) &= 2(D_k f)(x) + x\Delta f - k \frac{\partial(xf)}{x_2 \partial x_2} - k \frac{e_2 f}{x_2} + k \frac{Q(xf)e_2}{x_2^2} + k \frac{f'e_2}{x_2} \\ &= 2(M_k f)(x) + xM_k \bar{M}_k f - 2k \frac{Q'f}{x_2} + k \frac{f'e_2 - e_2 f}{x_2}. \end{aligned}$$

Thus the result holds by lemma 7.1.3.

Theorem 7.1.21 *The set of hyperbolic harmonic functions is left and right complex vector space.*

Theorem 7.1.22 *Let $f : \Omega \rightarrow \mathbb{H}$ be twice continuously differentiable. Then f is k -hypermonogenic if and only if f and xf are k -hyperbolic harmonic functions.*

Chapter 8

Interactive tools

Two interactive tools were designed using *Matlab* for this study.

- An user interface that aids in visualizing and understanding the transformation of the spheres - Euclidean and hyperbolic.
- An user interface to locate the center of a hyperbolic sphere.

As the user varies the design conditions in the Graphical User Interface(GUI), the corresponding geometry is sketched.

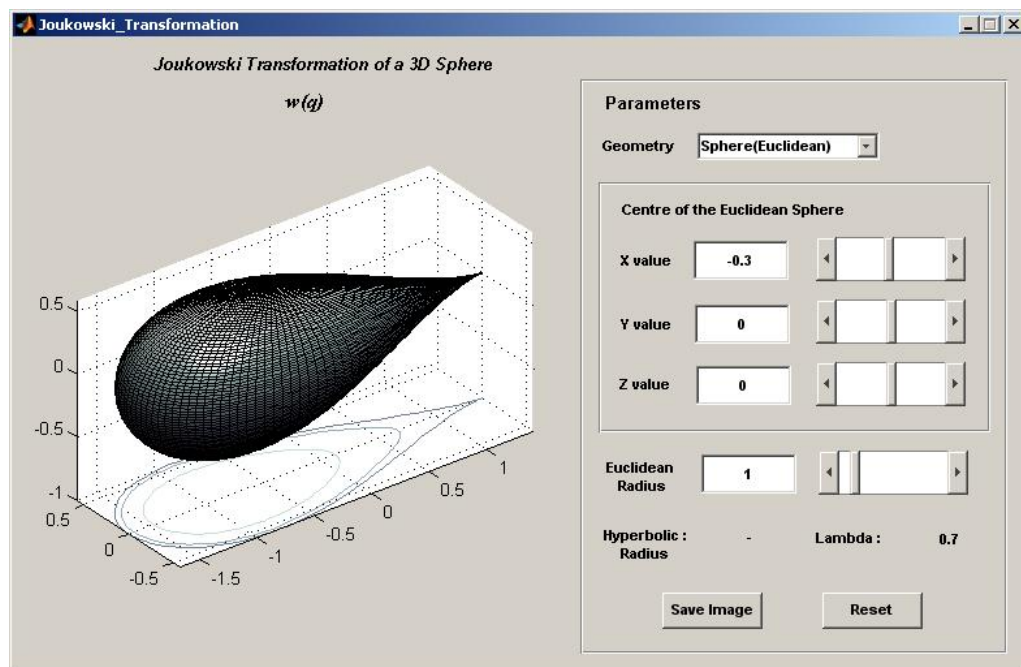


Figure 8.1: A Graphical User Interface to sketch the geometries of the mapping function

The *Graphical User Interface* in figure 8.1 has the following features:

Geometry - A drop down list box that allows the user to select between the Euclidean and hyperbolic sphere.

Euclidean Radius - A text box and slider that enables the user to enter the radius of an Euclidean sphere. Its default value is set to 1.

Hyperbolic Radius - The hyperbolic radius is calculated for a hyperbolic ball based on the Euclidean radius entered by the user and it is shown here.

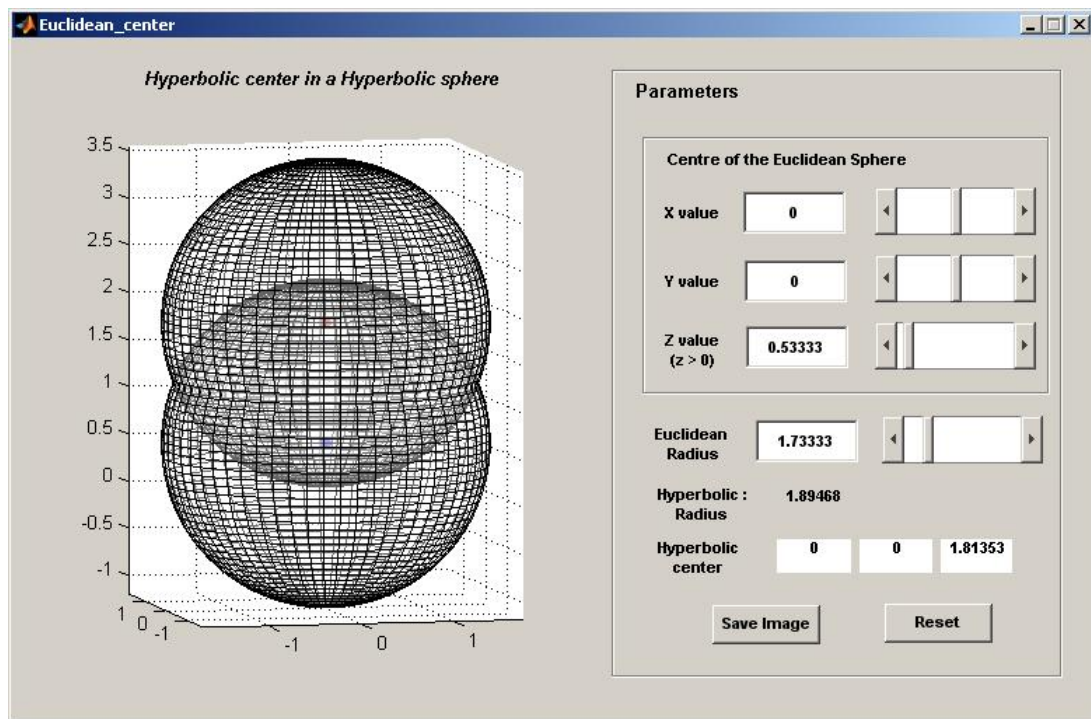


Figure 8.2: An User Interface that shows the movement of the center in a hyperbolic ball. The non-Euclidean center is shown using a 'red' marker.

Center of the sphere - This panel allows the user to change the co-ordinates of an Euclidean sphere. The input can be entered either using the text boxes or the sliders.

Note: Recall that the z co-ordinate for a hyperbolic sphere is strictly greater than 0 and the center of a hyperbolic sphere is not the same as the centre of an Euclidean sphere.

- X value represents the x co-ordinate of a sphere.
- Y value represents the y co-ordinate of a sphere.

- *Z value* represents the z co-ordinate of a sphere.

lambda - This is the transformation parameter λ calculated from the value of the radius and the centre of a sphere.

Save Image - It is a push button to save the image of a geometric shape.

Reset - Another push button that allows the user to reset the parameters of the images to their default values. In other words it resets a geometric shape to its default view.

3D Rotation - This feature enables the user to rotate an image to any orientation using the mouse. By right-clicking on the image the context menu appears. This includes the menu item *Rotation options*. After an option is selected from the sub-menu, the image can be rotated by pressing and holding down the mouse button.

In addition, the context menu also includes the following items:

- *Reset to Original Menu* This resets the image to the default view.
- *Go to xy view* A view of the image along the Z axis.
- *Go to xz view* A view of the image along the Y axis.
- *Go to yz view* A view of the image along the X axis.

The Interactive tool in figure 8.2 plots the location of a non-Euclidean center in a hyperbolic sphere and includes most of the features of user interface in figure 8.1.

Chapter 9

Conclusion

The present study was to determine the properties of a hypercomplex Joukowski transformation. The shapes deduced from both the Euclidean and Non-Euclidean geometries are intriguing. In comparison the mapping function for an Euclidean geometry does have similarities with the 2-dimensional profile except for the case when the parameter λ equals the radius of the sphere. Furthermore, the hyperbolic geometry renders a different view altogether with shapes evolving from variations in the final co-ordinate axis.

The highlight of the hypercomplex map is the airfoils in three dimensions. No modifications are needed in the spherical co-ordinates to generate the airfoil shapes which is unlike the profile in \mathbb{R}^3 (4.9). Besides this, cambered airfoils can also be constructed using this hypercomplex function.

From an application standpoint, the question remains ‘can these results address the issues of real-life?’ In simple words, to know if the airfoil shapes generated by using quaternions can be used. It is known that systematic methods are employed in developing airfoils in the aviation sector. These techniques are tailor-made to meet certain requirements and are not disclosed publicly. However, further experimental investigations to compare these methods including the proposed mapping function in this study might provide some useful insights into these complicated geometries. Moreover, it is an opportunity to find out if this method can be used as a replacement as well, thus opening up future work.

Quaternions, until now have been considered to be less intricate. Now with their appearance in a classic mathematical technique, they could even shed light on some of the methods applied in the aviation world.

On second thoughts, the airfoils produced can be treated as streamlined objects and not just as cross sectional shapes. This provokes more interesting questions and the areas where they can be implemented. Probably the list could begin from the design

of stream locomotives such as solar vehicles.

To conclude, the transformation functions (5.2) and (6.11) also find themselves as hypermonogenic functions. Plus, these equations are noticed to route to a system (7.3) that are commonly used in fluid flow or electrostatics.

Bibliography

- [1] Ira H. Abbott and Albert E. Von Doenhoff, *Theory of wing sections including a Summary of Airfoil Data*, Dover publications, 1959.
- [2] John D. Anderson, *Fundamentals of Aerodynamics*, New York: McGraw-Hill, 1984.
- [3] Thomas J. Benson, *Interactive Educational Tool for Classical Airfoil theory*. Cleveland, Ohio: NASA Lewis Research Center, Oct 30, 1996.
<http://www.grc.nasa.gov/WWW/K-12/airplane/FoilTheory.pdf>.
- [4] Tom Benson, Conformal Mapping: *Joukowski Transformation*, Glenn Research Center, National Aeronautics and Space Administration.
<http://www.grc.nasa.gov/WWW/K-12/airplane/map.html>.
- [5] Tom Benson, *Wing geometry definitions*, Glenn Research Center, National Aeronautics and Space Administration.
<http://www.grc.nasa.gov/WWW/k-12/airplane/geom.html>.
- [6] S.-L. Eriksson-Bique, Hyperholomorphic functions in \mathbb{R}^3 , *Clifford algebras and potential theory*, edited by S.-L. Eriksson, University of Joensuu, 2004.
- [7] Stephen Garber, *Airfoil Diagram*, U.S. Centennial of Flight Commission.
www.centennialofflight.gov/essay/Dictionary/angleofattack/D15.htm.
- [8] Stephen Garber, *Subsonic Airflow Effects - Airfoils and Wings*, U.S. Centennial of Flight Commission.
http://www.centennialofflight.gov/essay/Theories_of_Flight/Airfoils/TH13.htm.
- [9] Dario Isola, *Joukowski Airfoil Transformation*. MATLAB Central.
<http://www.mathworks.com/matlabcentral/fileexchange/loadFile.do?objectId=8870>.

- [10] Nitin R.Kapania, Katherine Terracciano, Shannon Taylor, *Modeling the Fluid flow around Airfoils using Conformal mapping*, Aug 29, 2008.
www.siam.org/students/siuro/vol1issue2/S01010.pdf.
- [11] H.Leutwiler, Lecture notes on Hyperbolic harmonic functions and their function theory: *Clifford algebras and potential theory*, edited by S.-L. Eriksson, University of Joensuu, 2004.
- [12] H.Leutwiler, Introduction to Generalized Function theory, *Clifford algebras and potential theory*, edited by S.-L. Eriksson, University of Joensuu, 2004.
- [13] H.Leutwiler, Modified Clifford Analysis in, *Complex Variables*, Theory Appl. 17 (1992), pp 153-171.
- [14] H.R. Malonek, R. De Almeida, *A note on a generalized Joukowski transformation*, Elsevier 2010.
- [15] H.R. Malonek, Selected topics in hypercomplex function theory in *Clifford algebras and potential theory*, edited by S.-L. Eriksson, University of Joensuu, 2004.
- [16] Z.Nehari, *Conformal Mapping*, first edition. New York: McGraw-Hill, 1952.
- [17] Peter J.Olver, Lecture notes on Complex analysis and Conformal mappings.
www.math.umn.edu/~olver/pd/cm.pdf.
- [18] Heikki Orelma, *New Perspectives in Hyperbolic Function Theory*, Tampere University of Technology, May 2010.
- [19] Evelyn Sander, *Models of Hyperbolic plane*, The Geometry Center, University of Minnesota. <http://www.geom.uiuc.edu/docs/forum/hype/model.html>.
- [20] Ken Shoemake, *Notes on Quaternions*. Dept. of Computer and Information Science, University of Pennsylvania.
www.cs.caltech.edu/courses/cs/171/quatut.pdf.
- [21] Tony Sudbery, Introduction to Quaternions in: *Clifford algebras and potential theory*, edited by S.-L. Eriksson, University of Joensuu, 2004.
- [22] Simo Särkkä, *Notes on Quaternions*, 2007.
www.lce.hut.fi/~ssarkka/pub/quat.pdf.
- [23] Paul Walsh. *Introduction to Conformal Mapping in Aerodynamics*. Dept. of Aerospace Engineering, Ryerson University.
www.ryerson.ca/p3walsh/aero504/conformal.doc.

Appendix A

M-files

In this chapter, the source codes written using *Matlab* for this study are included. The values used in the transformation functions (4.16) and (6.11) to plot the *airfoils* are tabulated at the end.

A.1 Joukowski profile in 2-dimension

```
close all;
clear all;
clc;

disp('Centre of the circle');
c1 = input('x coordinate: ');
c2 = input('y coordinate: ');
b = input('radius of the circle: ');

c = c1+1i*c2;
angle = linspace(0,2*pi,1000);

lambda = b - abs(c);

z = b*(cos(angle)+ 1i*sin(angle)) + c;

figure(1)
plot(real(z),imag(z), 'LineWidth',2)
axis([-3 3 -3 3])
grid on

J = z + lambda^2./z; % Joukowski Transformation

figure(2)
plot(real(J),imag(J), 'LineWidth',2, 'Color', 'k')
grid on
axis([-5 5 -3 3])
```

A.2 Joukowski profile in \mathbb{R}^{m+1}

This program handles the case for $m = 2$ in (4.8) and three variations of the spherical co-ordinates are used. Case I generates the shapes mentioned in the proposition 4.3.1 and case II and III yields airfoils in three dimensions.

```

%% CASE I
opengl neverselect;
clear all;
close all;
clc;

numfaces = 100;

phi = linspace(0,2*pi,numfaces);
theta = linspace(0,pi,numfaces);
[phi,theta] = meshgrid(phi,theta);

disp('Center/Origin of the sphere');
c1 = input('X Coordinate: ');
c2 = input('Y Coordinate: ');
c3 = input('Z Coordinate: ');
r = input('Radius of the sphere: ');

x0 = r*sin(phi) + c1;
x1 = r*cos(phi).*cos(theta) + c2;
x2 = r*cos(phi).*sin(theta) + c3;

figure(1)
surf(x1,x2,x0);
colormap bone
lightangle(0,60)
axis equal

% Joukowski hypercomplex profile
w0 = 2/3*(r-1/r^2)*sin(phi);
w1 = 2/3*(r/2+1/r^2)*cos(phi).*cos(theta);
w2 = 2/3*(r/2+1/r^2)*cos(phi).*sin(theta);

figure(2)
surf(w0,w2,w1);
colormap bone
lightangle(0,60)
axis equal

%% CASE II

opengl neverselect;
clear all;
close all;
clc;

numfaces = 100;

```

```

phi = linspace(0,2*pi,numfaces);
theta = linspace(0,pi,numfaces);
[phi,theta] = meshgrid(phi,theta);

disp('Center/Origin of the sphere');
c1 = input('X Coordinate: ');
c2 = input('Y Coordinate: ');
c3 = input('Z Coordinate: ');
r = input('Radius of the sphere: ');

x0 = (1+r)*sin(phi) + c1;
x1 = -r+(1+r)*cos(phi).*cos(theta) + c2;
x2 = (1+r)*cos(phi).*sin(theta) + c3;

figure(1)
surf(x1,x2,x0);
colormap bone
lightangle(0, 60)
axis equal

v = (r^2+(1+r)^2-2*r*(1+r)*cos(phi).*cos(theta)).^(-3/2);

% Joukowski hypercomplex profile
w0 = 2/3*x0.*(1 - v);
w1 = 2/3*x1.*(0.5 + v);
w2 = 2/3*x2.*(0.5 + v);

figure(2)
surf(w0,w2,w1);
colormap bone
lightangle(0,60)
axis equal

%% CASE III

opengl neverselect;
clear all;
close all;
clc;

numfaces = 100;

phi = linspace(0,2*pi,numfaces);
theta = linspace(0,pi,numfaces);
[phi,theta] = meshgrid(phi,theta);

disp('Center/Origin of the sphere');
c1 = input('X Coordinate: ');
c2 = input('Y Coordinate: ');
c3 = input('Z Coordinate: ');
r = input('Radius of the sphere: ');

x0 = (1+r)*sin(phi)+ c1;
x1 = (1+r)*cos(phi).*cos(theta) + c2;
x2 = -r+(1+r)*cos(phi).*sin(theta) + c3;

```



```

figure(1)
surfc(x1,x2,x0);
colormap bone
lightangle(0, 60)
axis equal

v = (r^2+(1+r)^2-2*r*(1+r)*cos(phi).*sin(theta)).^(-3/2);

% Joukowski hypercomplex profile
w0 = 2/3*x0.*(1 - v);
w1 = 2/3*x1.*(0.5 + v);
w2 = 2/3*x2.*(0.5 + v);

figure(2)
surfc(w0,w2,w1);
colormap bone
lightangle(0,60)
axis equal

```

A.3 Joukowski profile - Euclidean

The program below plots the Joukowski transformations for an Euclidean sphere.

```

opengl neverselect;
clear all;
close all;
clc;

k = 1;
numfaces = 100;

disp('Coordinates of the sphere');
c1 = input('X coordinate: ');
c2 = input('Y coordinate: ');
c3 = input('Z coordinate: ');
r = input('Radius of the sphere: ');

phi = linspace(0,pi,numfaces);
theta = linspace(0,2*pi,numfaces);
[phi,theta] = meshgrid(phi,theta);

x1 = r*sin(phi).*cos(theta) + c1;
x2 = r*sin(phi).*sin(theta) + c2;
x3 = r*cos(phi) + c3;

subplot(1,2,1)
surfc(x1,x2,x3);
colormap bone
material shiny
lightangle(0, 60)

```

```

axis equal

lambda = r-sqrt(c1^2+c2^2+c3^2); % Transformation parameter

for i = 1:length(x1)
    for j = 1:length(x2)
        q(k,1) = x1(i,j);
        q(k,2) = x2(i,j);
        q(k,3) = x3(i,j);
        q(k,4) = 10e-6;

        % Joukowski transformation
        JTr = [q(k,1) q(k,2) q(k,3) q(k,4)]+lambda^2.*quatinv([q(k,1) q(k,2) q(k,3) ←
            q(k,4)]);

        J(k,1) = JTr(1);
        J(k,2) = JTr(2);
        J(k,3) = JTr(3);
        k = k + 1;
    end
end

p = 1;
for m = 1:numfaces
    for n = 1:numfaces
        JR(n,m) = J(p,1);
        p = p + 1;
    end
end

q = 1;
for m = 1:numfaces
    for n = 1:numfaces
        JIm1(n,m) = J(q,2);
        q = q + 1;
    end
end

s = 1;
for m = 1:numfaces
    for n = 1:numfaces
        JIm2(n,m) = J(s,3);
        s = s + 1;
    end
end

subplot(1,2,2)
surfc(JR,JIm1,JIm2);
colormap bone
material shiny
lightangle(0, 60)
axis equal

```

A.4 Joukowski profile - Hyperbolic

This program sketches the Joukowski transformations for a hyperbolic sphere.

```

opengl neverselect;
clear all;
close all;
clc;

k = 1;
numfaces = 100;

phi = linspace(0,pi,numfaces);
theta = linspace(0,2*pi,numfaces);
[phi,theta] = meshgrid(phi,theta);

disp('Coordinates of the sphere');
c1 = input('X coordinate: ');
c2 = input('Y coordinate: ');
c3 = input('Z coordinate(Z > 0): ');

while( c3 <= 0)
    c3 = input('Z Coordinate(Z > 0): ');
end

re = input('Euclidean radius: ');

rh = asinh(re/c3); % Hyperbolic radius
hc3 = c3*cosh(rh);

y1 = r*sin(phi).*cos(theta) - c1;
y2 = r*sin(phi).*sin(theta) - c2;
y3 = r*cos(phi) - hc3;

subplot(1,2,1)
surf(y1,y2,y3);
colormap summer
material shiny
lightangle(0,60)
axis equal

lambda = r - sqrt(c1^2 + c2^2 + hc3^2); % Transformation parameter

for i = 1:length(y1)
    for j = 1:length(y2)
        q(k,1) = y1(i,j);
        q(k,2) = y2(i,j);
        q(k,3) = y3(i,j);
        q(k,4) = 10e-6;

        % Joukowski Transformation
        JTr = [q(k,1) q(k,2) q(k,3) q(k,4)] + lambda^2*quatinv([q(k,1) q(k,2) q(k,3) ←
            q(k,4)]);
    end
end

```

```
J(k,1) = JTr(1);
J(k,2) = JTr(2);
J(k,3) = JTr(3);
k = k+1;
end
end

p = 1;
for m = 1:numfaces
    for n = 1:numfaces
        JR(n,m) = J(p,1);
        p = p+1;
    end
end

q = 1;
for m = 1:numfaces
    for n = 1:numfaces
        JIm1(n,m) = J(q,2);
        q = q+1;
    end
end

s = 1;
for m = 1:numfaces
    for n = 1:numfaces
        JIm2(n,m) = J(s,3);
        s = s+1;
    end
end

subplot(1,2,2)
surf(JR,JIm1,JIm2);
colormap summer
material shiny
lightangle(0,60)
axis equal
```

A.5 Non-Euclidean center

Below is the source code that plots the non-Euclidean center of a hyperbolic sphere. The Euclidean sphere along with its center is also drawn.

```

clear all;
close all;
clc;

numfaces = 100;
az = -13;
el = 6;

phi = linspace(0,pi,numfaces);
theta = linspace(0,2*pi,numfaces);
[phi,theta] = meshgrid(phi,theta);

disp('Co-ordinates of the sphere');
c1 = input('X coordinate: ');
c2 = input('Y coordinate: ');
c3 = input('Z coordinate: ');
r = input('Euclidean radius: ');

rh = asinh(r/c3); % Hyperbolic radius
hc3 = c3*cosh(rh);

% Hyperbolic sphere
x = r*sin(phi).*cos(theta) + c1;
y = r*sin(phi).*sin(theta) + c2;
z = r*cos(phi) + hc3;

% Euclidean sphere
ex = r*sin(phi).*cos(theta) + c1;
ey = r*sin(phi).*sin(theta) + c2;
ez = r*cos(phi) + c3;

figure(1)
surf(x,y,z);
colormap white
alpha(0.4)
hold on
scatter3(c1,c2,hc3,'ro','filled'); % Hyperbolic center
hold on
surf(ex,ey,ez);
colormap white
alpha(0.4)
hold on
scatter3(c1,c2,c3,'bo','filled');
rotate3d on
axis equal
view(az,el);

```

A.6 Test values

Table A.1: Euclidean sphere

Geometry	Euclidean radius	Parameter	Euclidean centre		
	r	λ	x	y	z
<i>Airfoil</i>					
Symmetric	1.35	1.05	0.3	0	0
Non-symmetric (positive camber)	1.3	0.983772	0.3	0	0.1
Non-symmetric (negative camber)	1.3	0.983772	0.3	0	-0.1

Table A.2: Hyperbolic sphere

Geometry	Euclidean radius	Parameter	Euclidean centre			
	r	r_h	λ	x	y	z
<i>Airfoil</i>						
Symmetric	1	0.362395	-1.88091	0	0	2.69993